CHALMERS

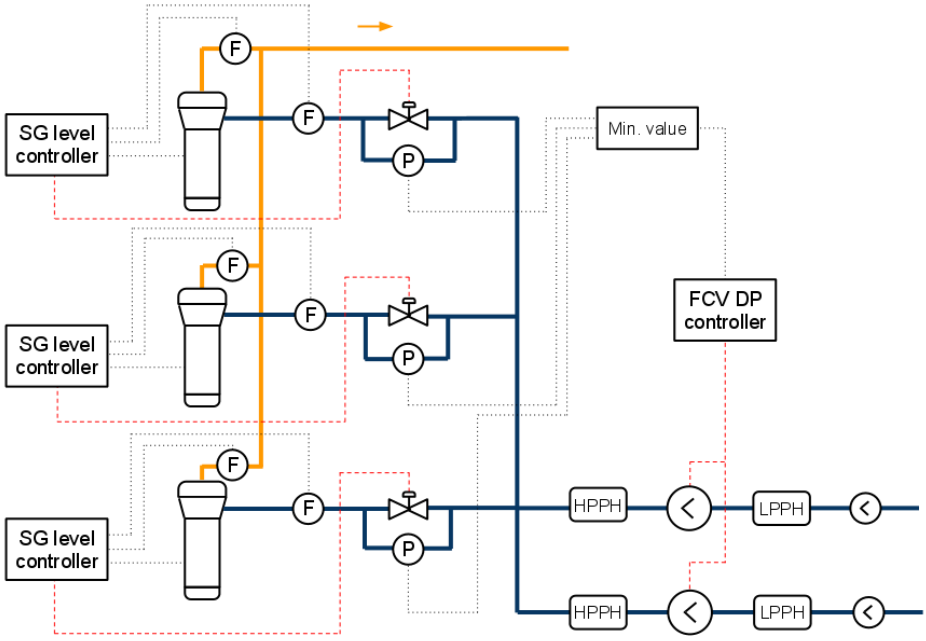


# Modelling and Control of Feed Water Systems in a Pressurized Water Reactor

*Master of Science Thesis*

CARL W. RESSEL

Department of Signals and Systems
*Division of Automatic Control, Automation and Mechatronics*
CHALMERS UNIVERSITY OF TECHNOLOGY
Göteborg, Sweden, 2010
Report No. EX074/2010

Modelling and Control of Feed Water Systems in a Pressurized Water Reactor

CARL W. RESSEL



Examiner: CLAES BREITHOLTZ

Chalmers University of Technology
Department of Signals and Systems
SE-412 96 Göteborg
Sweden
Telephone + 46 (0)31-772 1000

Supervisor: ANDERS EGEHOLM

Solvina AB
S-421 30 Västra Frölunda
Sweden
Telephone +46 (0)31-709 63 00

Cover: Overview of the feed water control system investigated in this report. For more information on the overview see chapter 1 page 7.

Department of Signals and Systems
Göteborg, Sweden November 2010

**Abstract**

The focus of this report is the feed water control system at reactor 3 in the Ringhals nuclear power plant. The current control system is a fairly simple combination of PID- and PI-controllers which has previously been determined to have room for improvement. The main goal of this project has thus been to find a suitable improvement strategy. By constructing a model of the plant, the control system has been evaluated and two main weaknesses were identified. The first weakness is a process coupling between two of the controllers and the second a difficulty to handle certain flow transients.

Initially a simple feed forward technique was evaluated with limited success. The main suggestion for improving the control system was instead found to be an MPC controller that could assist the current controllers. The suggestion was evaluated by designing the MPC controller and implementing it in the plant model. Simulation results indicated a small increase in system performance which could most likely be improved by further tuning of the controller.

**Acknowledgements**

I would like to express my gratitude to all the people who have been involved in this master thesis project. A special thanks goes to my supervisor at Solvina AB, M.Sc. Anders Egeholm for his support and suggestions during the span of the work.

I would also like to thank my examiner at Chalmers University of Technology, Prof. Claes Breitholtz for guidance and advice in key situations of the project.

At last a big thanks to all the people at Solvina AB who have been more than willing to help with all sorts of problems and questions, and of course for making my time there a pleasurable experience.

# Contents

# Nomenclature

## Abbreviations

| | |
|---|---|
| Dflow | Flow difference, specifically the difference between feed water flow and steam flow in the SG. |
| FCV | Flow Control Valve, specifically referred to the SG inlet FCV. |
| FCV DP | Differential Pressure over the Flow Control Valve. |
| HPPH | High Pressure Pre Heater. |
| LPPH | Low Pressure Pre Heater. |
| MPC | Model Predictive Control. |
| PI | Proportional and Integrative. |
| PID | Proportional, Integrative and Derivative. |
| PLS | Precautions, Limitations and Set points. |
| PWR | Pressurized Water Reactor. |
| QP | Quadratic Programming. |
| RC | Reactor Coolant. |
| RCP | Reactor Coolant Pump. |
| SG | Steam Generator. |
| SIMO | Single Input Multi Output. |

## Mathematical Symbols

| | |
|---|---|
| $\Delta p_p$ | Pressure difference over the feed water pump, $[bar]$. |
| $\Delta p_v$ | Pressure difference over a feed water control valve, $[bar]$. |
| $\Delta U$ | Vector of future control signals. |
| $\dot{x}$ | Time derivative of the state space variable. |
| $\phi$ | Feed water control valve position, $[rpm]$. |
| $\Psi_p$ | Feed water pump characteristic function. |
| $\Psi_v$ | Feed control valve characteristic function. |
| $\varnothing$ | Null matrix. |
| $A$ | Augmented model transition matrix. |

| | |
|---|---|
| $B$ | Augmented model input matrix. |
| $C$ | Augmented model output matrix. |
| $C_v$ | Feed water valve specific constant. |
| $H$ | Augmented model measurable output matrix. |
| $k_i$ | Sampling instant. |
| $K_{ob}$ | Kalman observer gain matrix. |
| $L_d$ | SG, downcomer water level, $[m]$ |
| $n$ | Feed water pump speed, $[rpm]$. |
| $N_c$ | Control horizon. |
| $N_p$ | Prediction horizon. |
| $Q$ | Model disturbance variance matrix. |
| $q_p$ | Feed water flow through a feed water pump, $[kg/s]$. |
| $q_v$ | Feed water flow through a feed water control valve, $[kg/s]$. |
| $R$ | Measurement disturbance variance matrix. |
| $s$ | Laplace operator. |
| $T_{mean}$ | Mean temperature in the RC loop. |
| $T_{ref}$ | Reference value form $T_mean$ calculated from turbine inlet pressure. |
| $V$ | Augmented model disturbance input matrix. |
| $x$ | State variable of the state space model. |
| $Y$ | Vector of predicted system output. |
| $\mathbf{I}$ | Identity matrix. |

# List of Figures

# Chapter 1

# Introduction

The aim of this chapter is to give an introduction of the project and to provide an overview of the topics presented in this report. The chapter will also contain more general topics such as the objective and purpose of the project.

## 1.1 Background

The main focus of this thesis is reactor 3 at the Ringhals nuclear power plant. The plant is of PWR-type (pressurized water reactor) which operates on the principle of using pressurized water as reactor coolant. The high pressure will prevent the coolant from boiling at high temperatures. The system can be divided into three separate, water based, heat transfer systems. The first system is the pressurized primary loop which is directly connected to the reactor and transfers heat from the core to steam generators (SG:s). The SG:s are then used to transfer heat to the second system which in turn powers the steam turbines. Once the steam has passed the turbines it's condensed back into water in the condensers, which are cooled with sea water from the third system.

The SG:s are basically big boiling pans where water from the second system is turned into steam. In order for the process to work as intended the internal water level is to be kept within defined levels at all times, independent of the steam out take. This requires a control system to regulate the feed water flow. The current system used at Ringhals 3 is a fairly simple cascade controller consisting of a PID- and PI-part regulating a flow control valve (FCV). In order to maintain a constant pressure over the FCV there is also a second PI-controller regulating the speed of the feed water pumps. As was shown in the research report by Bergdahl et al. [1] the current control system, although it meets the controller objectives, has a few drawbacks. The main problem was identified as the lack of communication between the controllers. An improved system performance could lead to less downtime such as reactor and turbine shutdowns which are often caused by ineffective feed water control as was shown in the paper by Zhao et al. [2].

By using a model of the plant the current system can be analyzed to see if there is a way to improve the SG water level control, which will be the main focus of this thesis project.

## 1.2 Objective

The main goal of this thesis project is to investigate how the overall performance of the feed water system at Ringhals 3 can be improved by the use of a more refined control strategy. The suggested solutions should be relatively easy to implement which means that they can only utilize measurements and actuators that are currently available in the real plant. The suggested controller should at least meet the control objectives imposed on the current system.

The construction and evaluation of a new control scheme will require a model of the feed water system. A secondary objective of the project will therefore be to extend an existing model of the power plant in order for it to be used as a base for the controller design.

## 1.3 Purpose

The rigorous safety and classifications systems surrounding the nuclear industry will most likely make it unfeasible to implement any large changes in the current controllers. However the result of this project could be used as an indication on what types of controllers might be appropriate to use in similar systems, which could prove to be valuable information for further research in the area. The project will also give a deeper insight into how the current control system will react in certain situations.

### 1.3.1 Educational purpose

The thesis project will also have an additional educational purpose as a finalization process for the master's degree. The project can be viewed as an opportunity to apply knowledge attained at both the bachelor and masters level to a real life engineering problem. During the span of the work the intention has also been to reach deeper into the field of multiple system control and process modelling techniques.

## 1.4 Delimitations

Several delimitations have been made to keep the project at a reasonable size, mainly considering the time frame of 15 weeks. Concerning the controller the main delimitation has been the assumption of a controller optimized for operation at nominal conditions (100% plant power level). This means that a fairly large part of problems associated with the lower power levels will not be taken into account. The delimitation will also simplify the controller to only handle disturbance rejection since the system has a fixed SG level reference value for power levels above 20 %, [3]. The project will also only cover the behavior at three types of disturbances, SG level set point changes, FCV DP set point changes and steam flow disturbances. These disturbances will cover most of the transients that the control system is designed for. At more severe disturbances automated safety systems will take control.

The scope of the simulation model has been kept at a reasonable level by excluding most of the systems which have a small or no impact on the feed water system. For example most of the turbine and condenser dynamics have not been included.

# Chapter 2

# Plant description

The aim of this chapter is to give an overview of the systems in the plant at Ringhals 3, it will also provide a deeper look into system dynamics of the parts related to the feed water system. The structure presented here will lay the foundation for the simulation modelling process presented in chapter 3.

## 2.1 Plant overview

The basic concept of a nuclear power plant is to generate electricity from the heat produced in nuclear processes. This is usually achieved by heating water into steam which can then be used to power steam turbines. The turbines will in turn power generators which produce electricity. As was mentioned in the introduction the plant at Ringhals 3 is of PWR type, which means that the reactor coolant is held under high pressure and does not come in direct contact with the turbines. Instead the reactor coolant acts as a middle step and is used to boil water in the steam generators (SG's). The reason for this type of design is mainly an increased level of safety. Here only the primary system together with the SG's need to be kept within the safety containment. It is thus highly unlikely that radioactive contamination would occur due to a breach on the secondary side. This also means that the turbines will have no contact with radioactive materials which will simplify maintenance.

The plant at Ringhals 3 consists of one reactor, one pressurizer, three SG's, two turbine lanes and two feed water lanes. An overview of the system can be found in figure 2.1. Since this project is aimed towards the SG's and feed water system the main focus will be put on these parts.

## 2.2 Primary system

The primary system consists of the reactor, pressurizer and reactor coolant pumps (RCP). All the energy that is extracted from the power plant is generated within the reactor. The fuel is held in a core assembly structure inside the reactor tank to allow for optimal heat transfer to the reactor coolant. The nominal (100%) thermal power of the reactor system at Ringhals 3 is 3144 MW from which about 9 MW is residual heat from the RCP's, [4]. The power level is controlled by inserting a set of control rods that will absorb neutrons that sustain the nuclear reaction. The level of absorption is determined by how far down the rods have been inserted.

In order to avoid boiling in the reactor coolant the pressure is to be kept well above the saturation level at all times. The primary loop is therefore equipped with a pressurizer that is capable of maintaining a pressure of 155.1 bar a at normal operating conditions, which gives a boiling point of 345 °C. The reactor coolant is passed though the SG's in three parallel loops each driven by its own RCP. The section of the loop going out reactor is called the hot leg and has a nominal temperature of about 323 °C. After passing the SG's the temperature is decreased to 284 °C and is returned to the reactor through the cold leg, [5]. The RC flow through each SG loop is about 4880 kg/s at 100% reactor power.

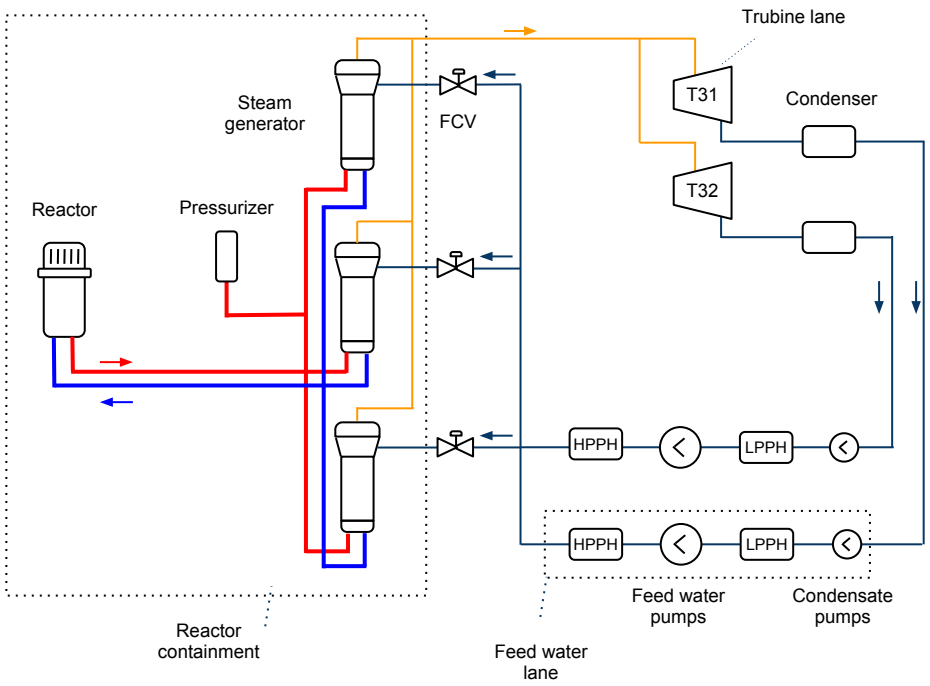


Figure 2.1: Overview of the plant at Ringhals 3.

## 2.3 Steam generators

The steam generators act as the intersection between the primary and secondary system. The SG's used at Ringhals 3 consists of 4 main parts, see figure 2.2. First the feed water from the secondary system enters the **downcomer** where it is mixed with the recirculation flow. The liquid is then heated in the **riser** after which it is passed through the **steam separator**. Here the steam is dried and passed to the **steam dome** at the top of the SG. The liquid is returned to the downcomer in the recirculation flow. The steam dome acts as a buffer to smoothen out fast pressure changes in case of steam outflow disturbances.

The SG's are based on a U-tube design where warm coolant from the primary loop is lead through a bundle of u-shaped tubes. These tubes are in turn surrounded by the cooler secondary side feed water in the riser which will lead to heat transfer between the two systems. The SG pressure will usually be around 62 bar, as oppose to 155.1 bar in the primary system, the increase in temperature will thus result in phase transitions from water to steam. During 100% power each SG will produce steam at a rate of up to 557 kg/s. In order to keep the water mass in the SG constant the feed water inlet flow has to be the same as the steam outlet flow. Values have been taken from the reactor and turbine PLS (Precautions, Limitations and Set points) documents, [5] and [3].

### 2.3.1 SG measurements

In order to achieve a good regulation of the SG water level a number of parameters have to be measured. The most important indicator of the water inventory in the SG is the downcomer water level. The level is measured in % of the narrow range, which is the level interval from the top of the U-tube bundle to the bottom of the steam separator, a difference of 4.85 m, [6]. This measurement is used, not only by the level controller, but also by several safety systems to protect the turbines and the reactor. Due to measurement disturbances the signal is filtered through a lag-filter before it enters the control system. The SG is also equipped with a wide range sensor that covers the full 16 m span. This measurement is however not used by the controllers.

Connected to each SG are also two flow sensors which are used by the level regulator. The sensors are used to measure the feed water inlet flow and the steam outlet flow from the SG. Both sensors work

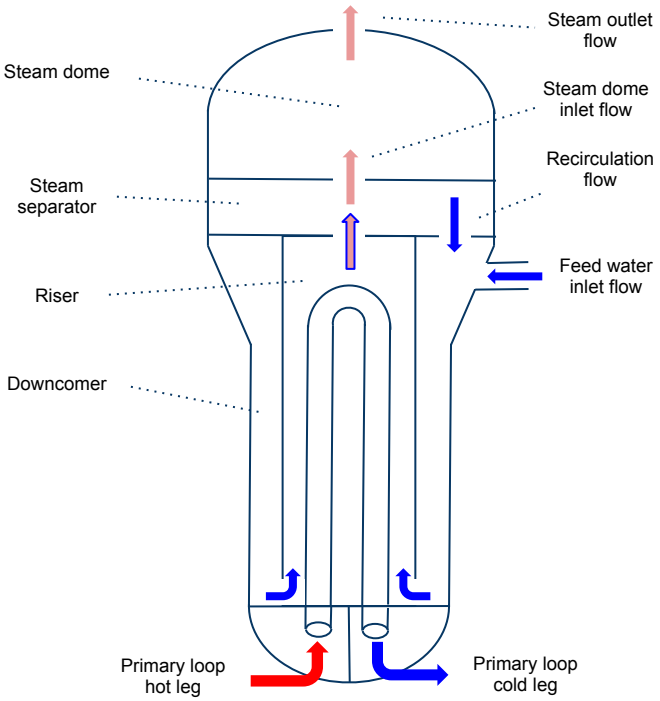


Figure 2.2: Simplified overview of an SG with four main parts; downcomer, riser, steam separator and steam dome.

on the principle of restricting the flow and then measuring the pressure difference over the restriction. In the case of the steam flow indicator we also need to know the density of the steam in order to get a mass flow measurement. This is not the case for the feed water flow indicator since the steam density, as opposed to the feed water density, will change significantly with pressure. The problem is solved simply by measuring the steam pressure in the SG which then can be used to calculate the steam density. The steam pressure measurement is also used in several safety systems to detect possible steam leeks. The flow indicators are optimized for nominal flow conditions and will produce relatively noisy signals for small flows. Information on the SG measuring system has been taken from the educational paper "Ånggeneratorernas reglering och mätning R3" [7].

### 2.3.2 Void collapse

Steam in the riser is formed as bubbles around the warm U-tube bundle and will rise to the top of the SG. A significant part of the complicated dynamics in the SG is due to these steam bubbles. Steam is, in contrast to liquid water, easy to compress and expand. When the SG pressure is increased the bubbles will be compressed. This will result in a rapid decrease in SG water volume and water level, even though the total water mass remains constant. This behaviour is usually referred to as "void collapse".

In a lot of cases these types of SG's will also experience void collapse response to an increase in feed water flow. The behavior is due to the decrease in riser temperature which follows the increased feed water flow. This effect has been shown to be most prominent at low power levels and will result in a non-minimum phase response of the system, meaning that the system will initially have an opposite reaction to a control parameter change.

However the SG's at Ringhals 3 have not shown any signs of non-minimum phase response, at least not in the higher power spectrum. The same conclusion was also reached in the research report by Bergdahl et al. [1] where it was stated that no non-minimum phase response could be observed in the power interval between 20% and 100%.

### 2.3.3 SG safety limits

The water level in the SG's is regulated to a certain value not only to allow for optimal steam production but also to sustain a high level of safety. If a break would occur on any of the pipes connected to the SG the steam or water will be dumped into the reactor containment. The water mass must thus be low enough so that even if all the water is turned into steam the containment safety pressure is not exceeded, [7].

There are however cases where the amount of water in the SG needs to be high enough to avoid an emergency shutdown of the reactor. Large transients, such as a power grid failure, will cause the turbines to rapidly decrease their power out take to about 5%, which is used to keep the power plant running. Steam from the SG's will in this case be dumped directly to the condensers to get rid of the excess energy while the reactor power is reduced with the control rods. There are however a small delay before the dump valves open which will cause the pressure to rise and the SG level to drop due to the void collapse. If the water level is low when this type of disturbance is introduced the level will run the risk dropping low enough to expose the U-tubes. There is however an auxiliary feed water system which will inject additional feed water into the SG once the level has dropped low enough. There is also an option to dump steam directly into the atmosphere to prevent high steam pressures.

## 2.4 Secondary system

The secondary system consists of two feed water lanes and two turbine lanes. The feed water lanes take water from the two condensers which is then preheated and fed to the SG's. The feed water lanes work in a parallel manner and are connected to a common pipe to which the SG FCV's are connected. Each lane has two condensate pumps which take water from the condenser. After this the feed water is passed through the low pressure pre heaters (LPPH) and mixed with drain flow from the turbines. The main feed water pumps, two in each lane, then increase the pressure to about 70 bar. The feed water is pre heated one last time in the high pressure pre heaters (HPPH) before it is mixed with the feed water from the other lane.

After the SG's the steam is again mixed into a common pipe from which the turbines take their inlet steam. The inlet flow to each turbine is regulated by a flow control valve to match the desired power output. Each turbine lane consists of 4 turbine steps, one high pressure turbine and three low pressure sections.

## 2.5 Control system overview

In order for the plant to operate as intended the system is equipped with an extensive control system. An overview of the main controllers related to this project is presented in this section. The main source of information concerning this subject has been the educational paper "Processreglering och skydd övergripande" [8].

### 2.5.1 Reactor/turbine interaction

The governing parameter for the reactor controller is the turbine power. This parameter is determined by measuring the inlet pressure (also referred to as impulse pressure) to the two turbine lanes which is then added and converted to a value called $T_{ref}$. $T_{ref}$ is used as a temperature reference for the mean temperature ($T_{mean}$) in the hot and cold legs. A $T_{ref}$ lower than $T_{mean}$ would indicate that the reactor is generating more energy than the turbines can use. This will cause the control rods to be inserted in order to reduce the nuclear reaction.

### 2.5.2 Steam dump control

As have been previously mentioned the plant is equipped with the capability of dumping excess steam directly to the condensers. This procedure is initiated to avoid emergency stops and allow for easy ramp up of the power level. The dump is controlled by three regulators; the steam pressure controller, the load reduction controller and the loss of load controller. The controllers are activated depending on what

state the plant is in. The steam pressure controller is mainly used when powering up and down the plant to regulate the SG steam pressure. The main regulator is the load reduction controller. If the difference between $T_{ref}$ and $T_{mean}$ is over 2 °C and the load reduction is greater than 10% the dump valves will be opened in proportion to the size of the reduction. The loss of load controller is activated in case of a reactor trip or an emergency stop of both turbines and will use the dump to regulate the reactor temperature to it's no load value of 292 °C.

### 2.5.3 Feed water control system overview

The control systems for the SG feed water flow can be divided into two sections, one regulating the FCV differential pressure (FCV DP) and one the SG water level. The plant is equipped with one FCV DP controller and three SG water level controllers (one for each SG). An overview of the control system can be seen in figure 2.3. These controllers will be investigated further in chapter 4.

The condensate pumps in the feed water lanes do not have dynamic controllers but are instead running with an on/off controller depending on flow and pressure at the suction side of the feed water pumps.

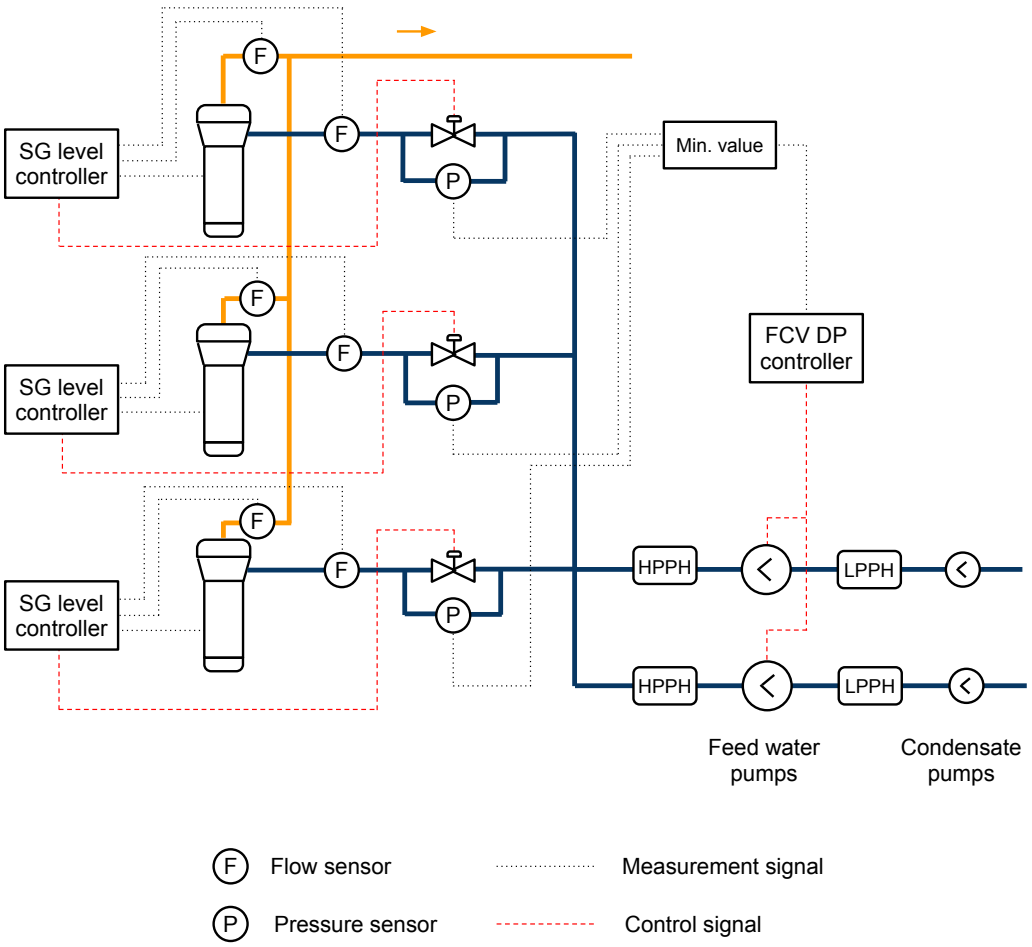


Figure 2.3: Overview of the FCV DP and SG level controllers.

# Chapter 3

# Simulation model

The aim of this chapter is to describe the modelling and validation process of the simulation model.

## 3.1 Model purpose/objective

The goal of the model presented in this chapter is to simulate the behavior of the power plant. The purpose of these simulations is to investigate how the real plant might be affected by changes in the control system. There is thus no tight restriction in model complexity or general computational demands. The model should be able to accurately describe the plant dynamics following certain induced disturbances.

## 3.2 Existing model

The base model used in this thesis is the simulation model developed by Andreas Nordquist during his master thesis "Dynamic modelling of a nuclear reactor system", [9]. The Nordquist model describes the Ringhals 3 plant prior to a recent upgrade from 3000 to 3144 MW thermal power. Even though the main focus of the model is the primary system it does contain both parts of the feed water and turbine lanes. There is however a need to adjust and extend the model in order for it to meet the demands posed by this project.

### 3.2.1 Modelica modelling language

The Nordquist model was developed in the simulation software Dymola, which in turn is based on the modelling language Modelica. Modelica is a object oriented simulation language which has more similarities to other object oriented languages such as C++ than classical simulation software such as MATLAB Simulink. The thing that differs Modelica from standard languages is the way equations are interpreted by the compiler. Rather than working with assignments as in the case of "$y := 3x$" where $y$ will be assigned the value of $3x$, Modelica works with equalities. The code $y = 3x$ can thus be interpreted as both "$y = 3x$" and "$x = \frac{1}{3}y$" depending on the evaluation order picked by the solver. This means that more complex equations can be written in plain form and the task of finding a solution is left to the solver. There are however ways to write assignment equations in Modelica by using a declaration called "algorithm" as opposed to the standard "equation" one.

The basic idea behind Dymola is that large models should be easy to construct using pre-existing models as building blocks. The components developed in Dyomla are therefore equipped with a graphical representation to allow for an easy overview when used in a larger model. There is also a standardized interface structure to determine how models can be connected to each other.

### 3.2.2 Model overview

The graphical representation of the plant in the Dymola model can be seen in figure 3.1. We see that the model consists of several connected sub models. The control system for the plant is implemented using a bus interface through which all the control signals are routed. The main reason behind separating

the plant and the control system is to allow for an easy overview of the system. Several simplifications are made in the model, for example the condensers have not been included. Since this thesis is mostly concerned with the interaction between the feed water pumps, FCV's and SG's this will not pose any problems.

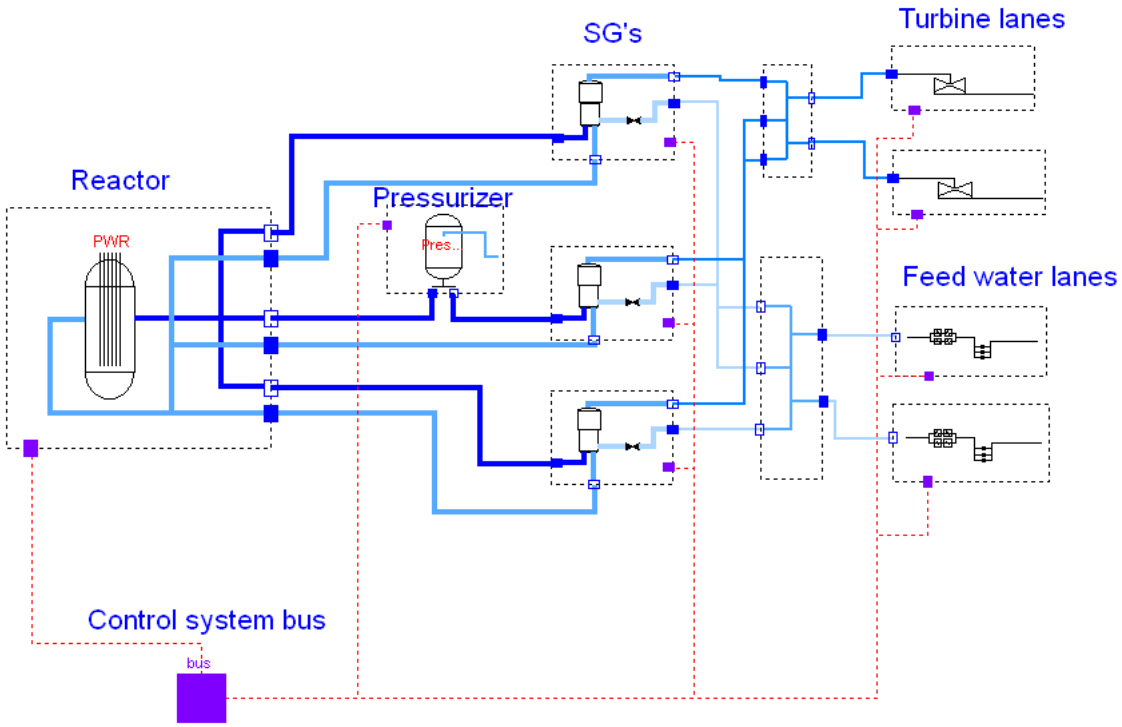


Figure 3.1: Plant overview in the Dymola model.

### 3.2.3 SG model

The SG's are modelled using a method based on discretization of the heat transfer elements. Both the U-tube bundle and the riser itself have been divided into small sections. Each section of the riser corresponds to one section of the upcoming part of the U-tubes and one of the downcoming part. Heat is transferred to the riser section depending on the temperature difference between the sections. The steam separator and downcomer are modelled as simple pipes with internal friction. Steam and liquid are separated in an ideally stirred tank where the liquid is recirculated to the downcomer together with the inlet flow.

### 3.2.4 Pump model

The pump dynamics is modelled using the pump characteristic function ($\Psi_p$) which describes the pumps ability to increase pressure and generate flow at a specific speed. The pump characteristics for the feed water pumps in the plant is given as a curve describing the flow to pressure relation during a nominal speed ($n_0$). This curve can then be shifted to suit other pump speeds using the pump affinity laws. The basic principle of the model is to generate a pressure difference ($\Delta p_p$) and let the other parts in the path determine a flow ($q_p$), this derivation is done automatically by the Dymola solver. The flow is then used to determine a new pressure difference over the pump using the pump characteristics (see equation (3.1)). The pump motor is modelled as a simple rotational mass with inertia $T_m$ and control input $u_n$,

equation (3.2).

$$\Delta p_p = \frac{n}{n_0}\Psi_p\left(q_p, \left(\frac{n}{n_0}\right)^2\right). \tag{3.1}$$

$$\dot{n} = \frac{1}{T_m}(u_n - n) \tag{3.2}$$

### 3.2.5 FCV model

The FCV determine the feed water flow depending on 3 things; the valve opening ($\varphi$), the pressure difference over the valve ($\Delta p_v$) and the water density ($\rho_v$). Just as in the case of the feed water pumps the FCV's have a valve characteristic function ($\Psi_v$) which describes how changes in valve opening will affect the flow ($q_v$). This can be formulated as

$$q_v = C_v \Psi_v(\varphi)\sqrt{\rho_v \Delta p_v} \tag{3.3}$$

where $C_v$ is a valve specific constant and $\Delta p_v \geq 0$. The valve opening is modelled as an accelerating mass up to the point of reaching a specified maximum rate of change, at which the rate of change is held constant. This means that the valve will have a nonlinear behavior in valve opening as soon as the rate limit is reached. The static friction of the mechanical parts of the valve has not been included in the model.

## 3.3 Model adaptations

The changes made in the model have been done in two steps. First the model has been updated with new parameters to be accurate at the higher power level of 3144 MW. The second step has been to extend some of the parts in close connection to the feed water control. Most of the new parameters have been taken from the Reactor and Turbine PLS as well as from measurement data attained from Ringhals 3, [5] and [3].

### 3.3.1 Feed water lanes

The feed water lanes have been extended with an additional LPPH (E109) which was added to the plant during the upgrade to the new power level. The two LPPH's have been implemented as one single unit in the model. In the Nordquist model the feed water pumps and the condensate pumps where both represented with a single pump unit each. The flow was then scaled to match the outputs of two pump units. This meant that it was impossible to stop one of the feed water pumps while the other one was running (which is the case in some situations). The model has therefore been extended with two separate feed water pumps and 3 condensate pumps. The pumps have also been modified with a check valve to stop any back flow while the pump is not running. A logic controller has been added to the condensate pumps to start the third pump depending on the pressure at the suction side of the feed water pumps. The new feed water lane can be seen in figure 3.2.

The pumps and heaters have also been given new parameters to reflect the changes in the plant.

### 3.3.2 Condensers

The condensers are not included in the Nordquist model which means that some of the dynamics concerning the control of the feed water pumps is missing. The most relevant part of the condenser system is the condenser controller which will even out imbalance between the two condensers by giving a small rpm offset to the feed water pumps. Since we have no accurate models of the turbines it will not be meaningful to make very accurate physical model of the condensers. The goal is instead to incorporate the effect of the condenser controller without actually modelling the physical system using the detailed Modelica objects. This has been done by a simple "mathematical" model where all the in and out flows to a certain condenser have been added and converted into water levels. Once we have the water level it is then simple to add a PI-controller to get the effect of the condenser controller.

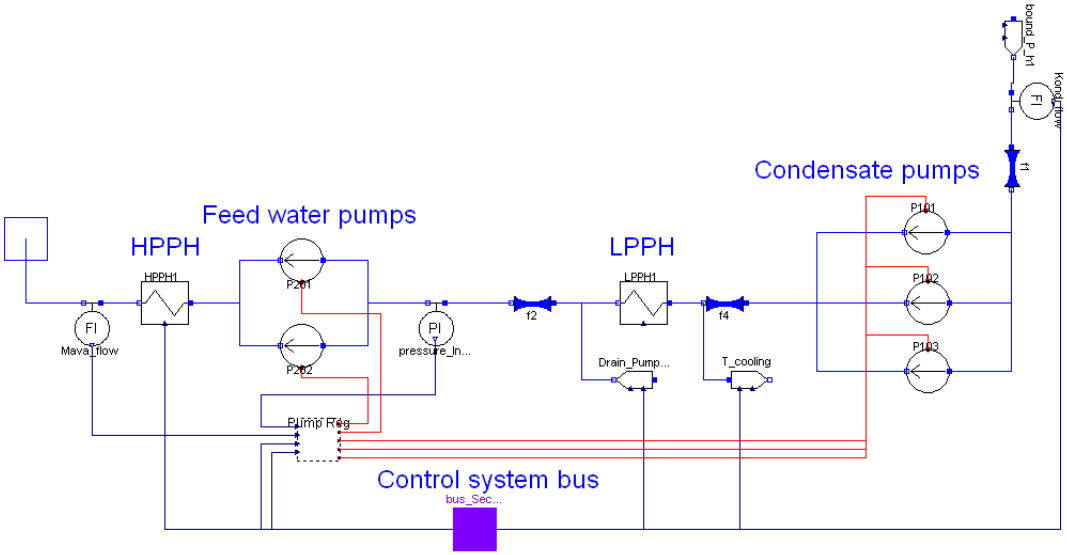


Figure 3.2: Dymola model of a feed water lane.

## 3.4 Model validation

The model has been validated against measurement data from the real plant. Three types of disturbances have been used during the validation process, DP steps, SG level steps and steam flow disturbances. In this case the steam flow disturbance is represented by a 50% load rejection transient, which is an instantaneous loss of load in the generators. The original Nordquist model was also validated against data from a house load transient which was presented in the Model validation report [10]. A house load transient is equivalent to a 100% load rejection case where both turbines stop. The reason for not validating against the same type of transient in this case was the lack of measurement data from the new system for such a scenario, at the time of writing this report.

Since the plant is modelled with three identical SG's only values from one SG are used in the validation. The measurement data has in most cases been calculated as a mean of the 3 SG's to remove noise and present that average behavior.

### 3.4.1 FCV DP step

Step changes in FCV DP are used to evaluate the DP-controller and to see if a change in FCV DP affects the plant in the correct way. The disturbance is induced as a reference step to the DP controller, and is made up of two steps. One from 8.2 to 10.4 bar at $t = 200$ s and one from 10.4 to 8.2 bar $t = 831$ s. The reason for not doing the step from 8 to 10 bar is the wish to match the simulated scenario with the measured data.

The result of the simulation can be seen in figures 3.3 to 3.6. In figure 3.3 we can see that the simulated FCV DP corresponds well to the measured values. The oscillatory behavior in the measured FCV DP is due to static friction in the valve which has not been included in the model. The pump rpm graph (3.4) is also a good indication that the DP controller is working as intended, there are however spikes in the measured values that are not represented in the simulation. This is probably due to measurement noise. The DP change will also affect the SG water level due to the lack of communication between the controllers, this can be observed in figure 3.5. We see that the mean behavior of level is described in a good way during the disturbance. In figure 3.6 we can see the reaction of the SG level controller which will close the FCV to maintain the same feed water flow when the FCV DP is increased. It's difficult to see if the overshoot of the controller is accurate due to the lack of static friction in the model. It is however deemed to be within the limits of error for the project.

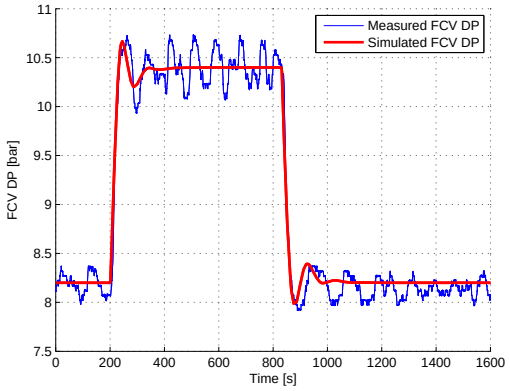


Figure 3.3: FCV DP during the FCV DP reference steps.

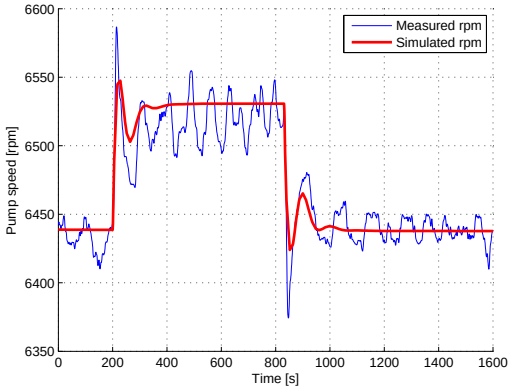


Figure 3.4: Feed water pump speed during the FCV DP reference steps.

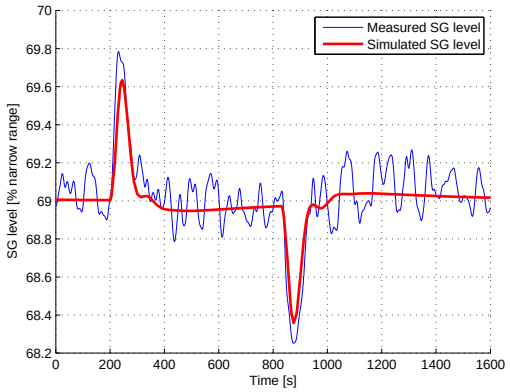


Figure 3.5: SG water level during the FCV DP reference steps.

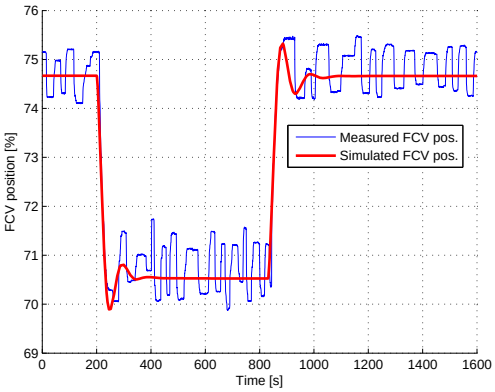


Figure 3.6: FCV position during the FCV DP reference steps.

### 3.4.2 SG level step

The main goal of the SG level step disturbance is to test the SG level controller. The disturbance is introduced as a reference change in the same way as the DP disturbance. Here the level reference value is changed from 69% to 66% at $t = 200$ s and back to 69% at $t = 1074$ s. The response in SG water level following such a reference steps can be seen in figure 3.7. We can here see that the simulation will generate values close to those of the real plant. The oscillations in the measured level are caused by noise in the sensors and static friction in the FCV which have not been included in the model.

The response in FCV position can be seen in figure 3.8. The simulated values differ significantly from the measurements in both the peak values and the overshoot. A reason for this could be a combination of lacking the FCV static friction and the lack of a model of the basic position controller in the FCV. As a result the FCV DP will also be too high which can be seen in figure 3.9. The high DP values might also be an effect of lag in the sensors which has not been included in the model. The resulting feed water flow from the FCV is still in good agreement with the measurements which can be seen in figure 3.10. The results are deemed satisfactory although further investigating into the mismatches might need to be done; there could for example be an error in the FCV opening/closing time constants.

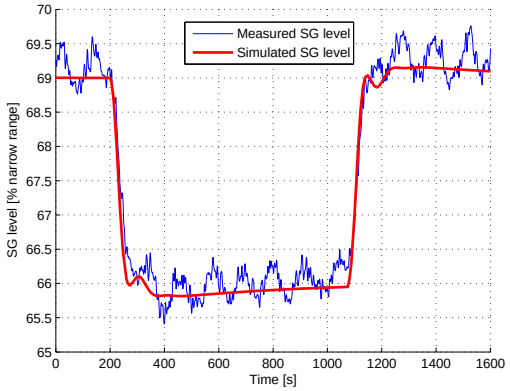


Figure 3.7: SG water level during the SG level reference steps.

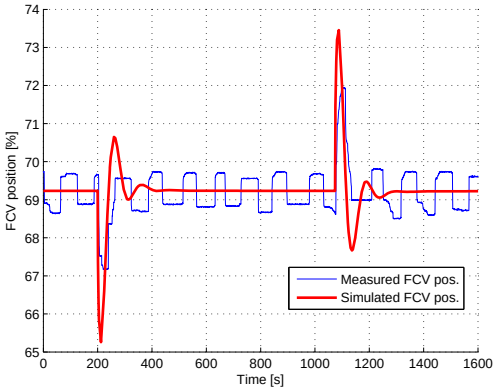


Figure 3.8: FCV position during the SG level reference steps.

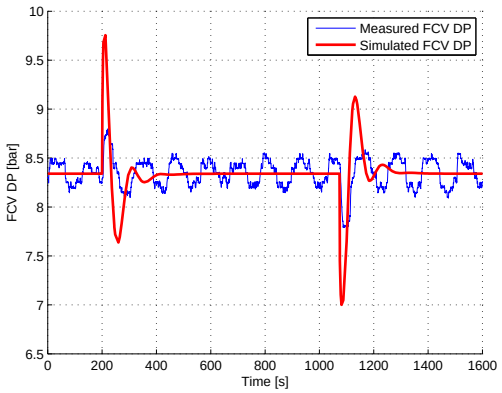


Figure 3.9: FCV differential pressure during the SG level reference steps.

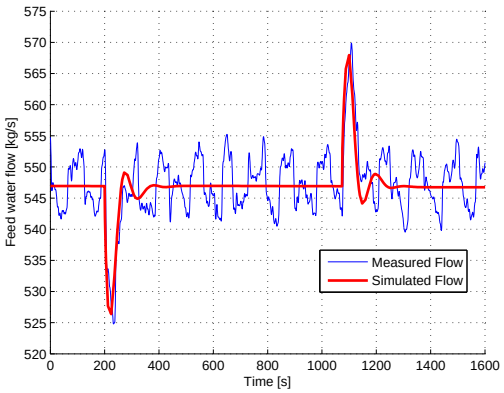


Figure 3.10: FCV feed water flow during the SG level reference steps.

### 3.4.3 Load rejection (50%)

The load rejection disturbance is used to validate the operation of the whole plant at the new power level and will incorporate most of the modelled systems. The disturbance is introduced as a reference step in one of the turbine power controllers at $t = 183$ s. This will cause the controller to close one of the turbines steam inlet valves which will generate a drop in the turbine impulse pressure and $T_{ref}$, see section 2.5.1. The loss of load controller will then react by opening the dump valves and inserting the control rods into the reactor core.

The SG water level during the disturbance will first drop due to void collapse and then rise again as soon as the dump is active. This behavior can be observed in figure 3.11. The second drop beginning at $t = 200$ s is due to the dump valves closing again. The simulation is able to describe the overall behavior of the level although there is a mismatch in amplitude for the two last peaks. This is probably due to some mismatch in the dump capacity.

The FCV position, DP and feed water flow during the disturbance can be seen in figure 3.12, 3.13 and 3.14. They all display values relatively close to those from the real plant. The conclusion from the validation is that the model can be used for designing a control scheme although one should keep the error margin in mind when analyzing the results.

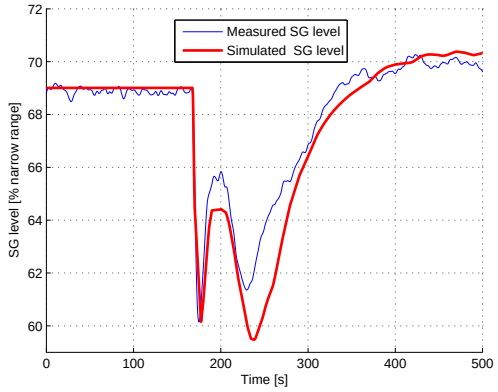


Figure 3.11: SG water level during the load rejection disturbance.

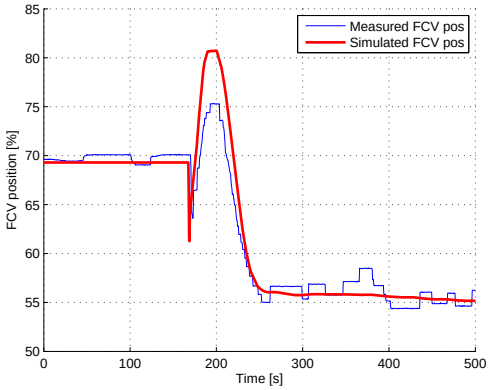


Figure 3.12: FCV position during the load rejection disturbance.

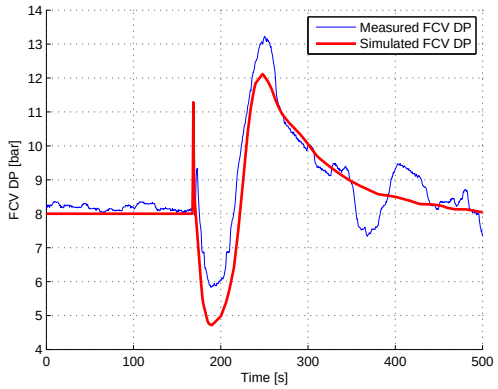


Figure 3.13: FCV differential pressure during the load rejection disturbance.

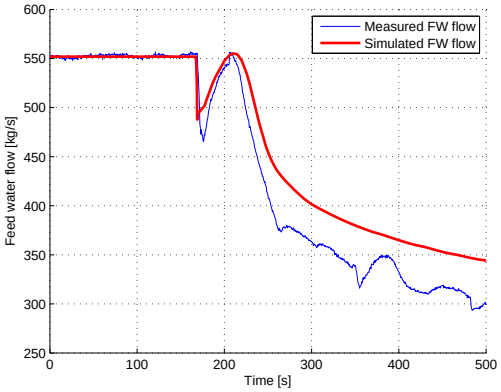


Figure 3.14: FCV feed water flow during the the load rejection disturbance.

# Chapter 4

# Feed water control system

The purpose of this chapter is to analyse the current control system at Ringhals 3 in order to find suitable improvement strategies.

## 4.1 FCV DP controller

The basic goal for the FCV DP controller is to keep the minimum FCV DP at 8 bar. The current strategy for controlling the FCV DP is, as was mentioned in the introduction, based on relatively simple control design. One PI-controller is used to maintain a minimum of 8 bar over the FCV's by regulating the feed water pump speed, see figure 4.1. The controller works with an input from a minimum value filter which picks out the minimum FCV DP from the three FCV's. The same output pump speed is then used to regulate the four feed water pumps, (two in each feed water lane). A Dymola representation of the controller can be found in appendix A.5. The controller is relatively fast with a time constant of 13 seconds, for a 2 bar reference step, [1].

The requirements on the controller are that the damping factor should be larger than 3 and the overshoot less than 30%, following a reference step increase of 2 bar, [11]. Here the damping factor is defined as the ratio between the amplitude above the reference value of the first overshoot and the second overshoot.

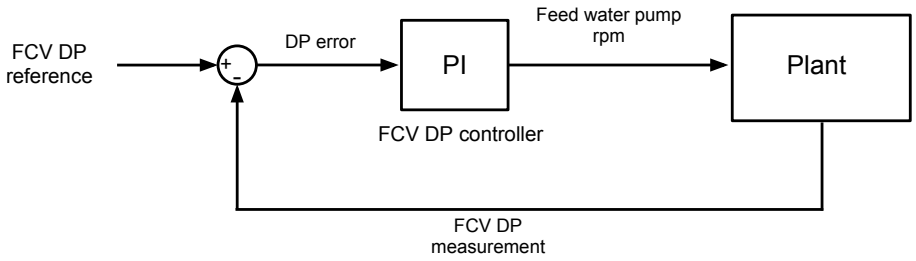


Figure 4.1: Closed loop overview of the FCV DP controller

## 4.2 SG level controller

The objective for the SG water level controller is to keep the water level in the SG at a specific reference value. The reference is fixed at 69% of the narrow range at reactor power levels above 20%. Under 20% the level reference follows a ramping program from 54% to 69%. Both the reference signal and the level measurement are filtered to remove noise, a procedure which will cause a small delay. In order for the controller to be able to react to fast changes in the steam flow there is also a feed forward of

the flow difference (Dflow) between inlet and outlet flow. The controller is therefore separated in two parts; one SG level compensator with a PID design and one SG flow compensator of PI design. The reference for the flow compensator is determined by the level compensator, see figure 4.2. The Dymola implementation of the controller can be found in appendix A.5.

The controller is required to have a damping factor (ratio between first and second overshoot) of more than 3 and a settling time ($t_{2\%}$) of less than 2 minutes, following a 3% reference step increase. Under nominal conditions the level fluctuation (min/max) should be less than 2.5%, [12].

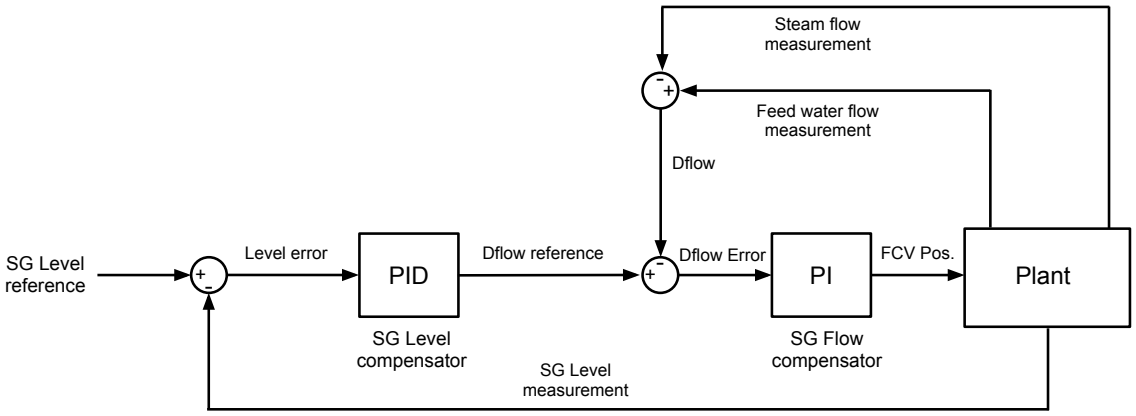


Figure 4.2: Closed loop overview of the SG level controller.

## 4.3 Control system analysis

As was mentioned in the introduction the main problem with the current control system is that the SG level controllers and the FCV DP controller are working as if they were separate systems even though there is a clear interconnection between them. As presented in the research report by Bergdahl et al. [1] the system might be open for improvement by the implementation of some more intricate controller strategy. The interconnection between the systems can be observed in figure 3.5 where a change in FCV DP reference caused the SG water level to spike.

There are however some benefits with the current system. For one the safety aspect of having several independent controllers means that if a single controller fails there is a chance that the remaining ones will still be able to keep their set points. The simple structure of the controllers also means that they are more likely to be tuned correctly by the operators.

### 4.3.1 Disturbance rejection

The main objective for both the FCV DP and SG level controllers is to keep a specific parameter as close to the reference as possible. For reactor power levels larger than 20% the references will be constant. The objective can thus be formulated as a disturbance rejection problem as opposed to reference tracking where the main problem is to follow a variable reference. The overall goal of the controllers is to keep the SG water level stable enough to avoid an emergency stop. By controlling the FCV DP to at least 8 bar we can make sure that there will be a possibility to increase the feed water flow during a transient. The value of 8 bar has been determined in order for the feed water system to handle certain scenarios.

In order to analyze how the current system operates two types of disturbances have been investigated, FCV DP disturbance and steam flow disturbance.

#### 4.3.1.1 FCV DP disturbance

A change in FCV DP will cause the feed water flow to change according to equation (3.3). Since the feed water flow is used in a feed forward design in the SG level controller (see figure 4.2) the controller

will react by manipulating the FCV opening. If the DP is increased the FCV will start closing, this will cause the FCV DP to increase even more until the DP controller has reduced the feed water pump rpm. Since there is no direct communication between the controllers the SG level controller has to wait for the feed water flow to change before it can react. Due to non ideal sensors there will be a delay in reaction before the FCV starts to close. This delay is the main reason behind the disturbance in the SG water level.

#### 4.3.1.2 Steam flow disturbance

The main problem with steam flow disturbances is that a sharp decrease in steam flow will result in an increased SG pressure. The increase in pressure will cause a void collapse that will result in a rapid drop in water level. We thus need to increase the total water mass in the SG to maintain a constant level.

The control system used today has a hard time to adapt to this type of disturbance, and will initially try to decrease the water mass. The effect of the disturbance on a few of the most interesting parameters can be seen in figure 4.3. First the fast SG flow compensator will detect a decrease in steam flow and close the FCV to maintain a zero flow difference (Dflow) between the feed water and steam flow. This will cause an increase in the FCV DP which in turn causes the DP controller to decrease the feed water pump speed. Since the SG level measurement is relatively slow it will take a few seconds before the SG level compensator will increase the flow reference (Dflow reference) to the flow compensator. At this point the flow compensator starts to open the FCV again but now the pump speed is decreasing which causes the FCV DP to drop rapidly. In the end the SG level compensator is able to stabilize the level after the transient. The main point here is that the controller's first action is made in the wrong "direction" which will worsen or at least prolong the impact of the disturbance.

There is however no controller that can eliminate this type of disturbance completely because of limitations in the physical system. Using an "optimal" controller, where the FCV opening and feed water pump speed will be set to their maximum values just after the disturbance, will still result in a SG level drop which can be seen in figure 4.4. The level will however not drop as low and it also returns faster to the reference value.

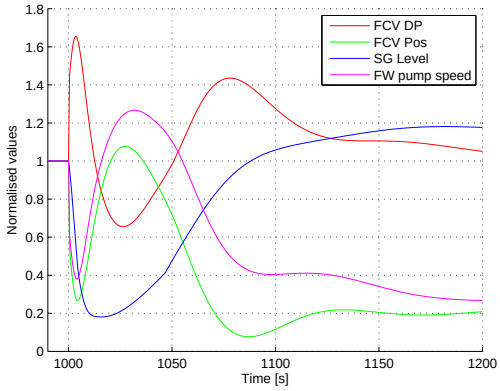


Figure 4.3: The effect of a 20% step decrease in steam flow at $t = 1000$ with the simplified simulation model in steady state. All values have been normalized to a steady state and max-min value of 1.

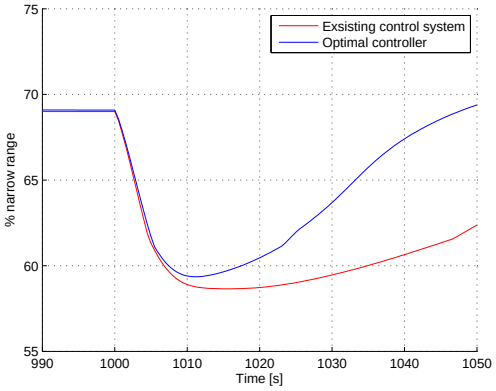


Figure 4.4: SG level initial fluctuations following a steam flow step decrease using the current controller vs. an "optimal" controller.

## 4.4 Control system improvements

There are a few cases in which the current control system can be improved as was shown in the previous section. The aim of this section is to present ways on how these improvements can be achieved. The most promising suggestion will be tested in the simulation model.

### 4.4.1 FCV DP feed forward

A solution suggested in the report by Bergdahl et al. [1] is to use the measurement of the FCV DP in feed forward setup to lessen the impact of a FCV DP disturbance on the SG level. This would solve the lack of communication problem between the controllers. The feed forward strategy is based on the concept of using a filtered version of a disturbance to cancel out its effects on the output, see figure 4.5. In this case the disturbance we want to cancel out is the FCV DP variations. In order to construct the feed forward filter ($F_f$) we need to isolate both the effect of the DP variations and the FCV position on the SG feed water flow. In other words to determine the linear $G_v$ and $G_u$ functions in figure 4.5.

From equation (3.3) we know that the flow will be proportional to the square root of the FCV DP ($\Delta p_v$).

$$q_v = C_v \Psi_v(\varphi)\sqrt{\rho_v \Delta p_v} = f_1(\varphi, \Delta p_v) \tag{4.1}$$

We start by approximating $f_1$ with a first order Taylor expansion around the steady state point ($\varphi_0$,$\Delta p_{v0}$).

$$q_v \approx f_1(\varphi_0, \Delta p_{v0}) + (\varphi - \varphi_0)\frac{\partial f_1}{\partial \varphi}\Big|_{\varphi_0, \Delta p_{v0}} + (\Delta p_v - \Delta p_{v0})\frac{\partial f_1}{\partial \Delta p_v}\Big|_{\varphi_0, \Delta p_{v0}} \tag{4.2}$$

By adding all the constants terms together to form $C_{ff}$, the equation can be rewritten as

$$q_v \approx C_{ff} + \varphi\frac{\partial f_1}{\partial \varphi}\Big|_{\varphi_0, \Delta p_{v0}} + \Delta p_v \frac{\partial f_1}{\partial \Delta p_v}\Big|_{\varphi_0, \Delta p_{v0}}. \tag{4.3}$$

The transfer function for the valve position system can be approximated as a simple first order system with time constant $1/\alpha$ as $G = \frac{\alpha}{s+\alpha}$. Using the terms from equation (4.3) we can now form the transfer functions $G_u$ and $G_v$ as

$$G_u = \frac{\alpha}{s+\alpha}\frac{\partial f_1}{\partial \varphi}\Big|_{\varphi_0, \Delta p_{v0}} \tag{4.4}$$

$$G_v = \frac{\partial f_1}{\partial \Delta p_v}\Big|_{\varphi_0, \Delta p_{v0}} \tag{4.5}$$

The goal is to cancel out the effects of changes in FCV DP on the feed water flow. The feed forward filter should thus be constructed in such a way that it will generate an opposite signal at the summation block inside the simplified FCV model for every change in FCV DP. The filter

$$F_f(s) = -\frac{G_v(s)}{G_u(s)} \tag{4.6}$$

will achieve this objective, [13]. Since the dynamic is fairly small, a viable approximate solution is to use only the static part of the function in the feed forward. The $F_f$ block can thus be calculated as

$$F_f(0) = -\frac{G_v(0)}{G_u(0)} = -0.49. \tag{4.7}$$

#### 4.4.1.1 FCV DP feed forward results

The feed forward design has been evaluated against the two disturbances presented earlier in section 4.3.1.1 and 4.3.1.2. In figure 4.6 we can see the effect on the SG water level during a FCV DP disturbance. The feed forward design is shown to be a significant improvement over the old system. The initial spike is almost completely removed and the following undershoot is nonexistent. The level is also returned to the steady state value much faster.

The second type of disturbance is the steam flow step. In figure 4.7 we can see that results are not nearly as encouraging. The SG water level drop due to the void collapse has increased and FCV DP is spiking in an oscillatory manner. The reason for the increased drop in SG level is the fact that some of the unwanted behavior is amplified by of the control system. When the SG flow compensator detects that the steam flow has decreased it will start to close the FCV, this will cause the FCV DP to increase. The increase in FCV DP means that the feed forward filter will close the FCV even further to maintain

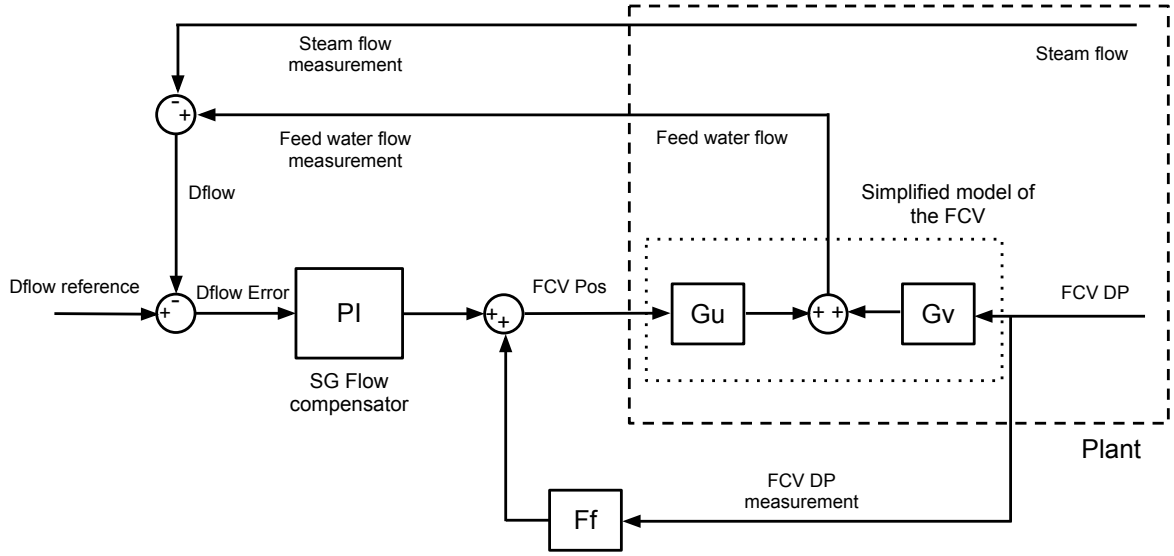


Figure 4.5: The basic concept of the DP feed forward design. The SG level compensator is here omitted.

a constant flow. This amplifying effect causes the SG level to drop to a lower level before the level controller reacts.

We can also see oscillations in the FCV DP which are originating from the amplifying connecting between the FCV position and the FCV DP. Part of the oscillations could probably be eliminated by reducing the sensitivity of the SG flow compensator. It is however clear that the FCV DP feed forward design will not be able to improve the system performance in the case of steam flow disturbance.

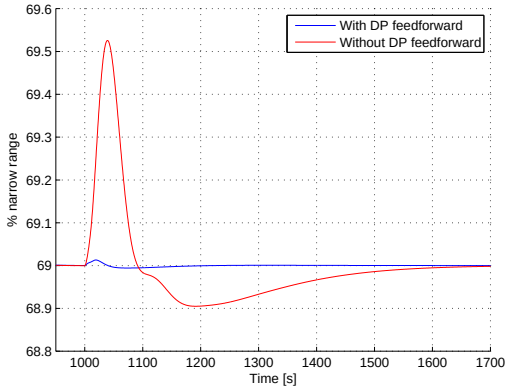


Figure 4.6: Variations in SG level during a step increase of FCV DP reference from 8 to 10 bar at $t = 1000$.

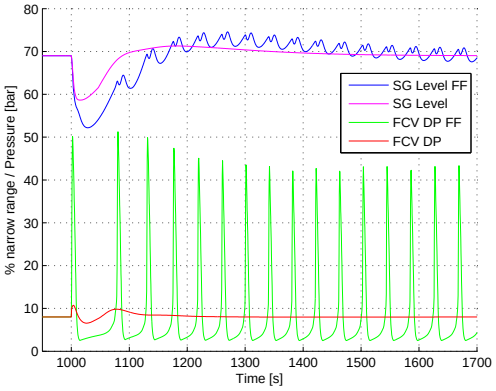


Figure 4.7: SG level and FCV DP during a step decrease in steam flow from 550 to 440 kg/s at $t = 1000$.

### 4.4.2 Multivariable controller

We saw in the previous section that a simple feed forward filter was not a viable option for improving the current control system. There are however other ways to attain a control system which could solve the lack out communication problem between the SG level controller and the FCV DP controller. Since the combined system has multiple control parameters (SG level and FCV DP) and multiple actuators (feed water pump rpm and FCV position) it is reasonable to suggest some kind of multivariable controller. The same conclusion was also reached in the report by Bergdahl et al. [1] where a specific mention was made to the use of decoupling filters.

Numerous papers have been published concerning the topic of SG level control, where a wide variety of controller techniques have been investigated, in particular controllers based on $H_\infty$ structures such as nonlinear $H_\infty$ by Parlos et al. [14] and switching $H_\infty$ controller based on Lyapunov functions by Hu et al. [15]. There have also been papers published with a more novel approach where techniques such as output feedback dissipation by Dong et al. [16] and partial feed forward with decoupling control by Liu et al. [17] have been evaluated.

These papers are however mainly focused on controlling the SG water level at instances where the non minimum phase behavior is present and by just regulating the feed water flow. Our case is a bit different since we can't control the feed water flow directly, we instead have to make use of the feed water pump rpm and FCV position, and there are also no indications of non minimum phase behavior in our case.

#### 4.4.2.1 Decoupling filter design

The basic idea behind a decoupling filter is to make parameters that would normally be affected by each other act as if there were no connection between them. This is accomplished by the use of an internal model from which the filter can predict the output response and thus compensate for any interconnection. In our case this would mean that the connection between the FCV DP and SG level could be eliminated. The major points for and against using a decoupling filter in this case are;

+ Would be able to greatly reduce the interactions between the FCV DP and the SG level. The decoupling could also be useful when the system is running in manual mode if for example the operator wants to manipulate only one parameter without affecting the other.

+ A design using a decoupling filter could make use of the existing controllers. The filter would just be added between the controllers and the control variables making it fairly easy to implement.

− The filter would only address the communication issue between the controllers and not the problems associated with the steam flow disturbance that we saw in section 4.3.1.2.

− Since the decoupling is made using a simple model of the plant the design would be sensitive to model errors. There will also be a need to update the model when even minor modifications are made in the plant.

The overall conclusion is that a decoupling filter could be suitable for removing the controller couplings but would not be able to improve the system performance during the steam flow disturbance.

#### 4.4.2.2 MPC controller

We previously saw that a feed forward of the measured FCV DP disturbance were able to eliminate most coupling effect between the controllers. The goal is thus to combine that effect in a controller that will also provide the appropriate response to a steam flow disturbance. We also want to keep most of the safety aspects present in the current system. A possible solution to this might be to implement a model predictive controller (MPC).

As can be heard from the name the MPC uses an internal model to predict the future state of for example the SG water level. The prediction can then be used to calculate an optimal control signal to regulate the system. The level fluctuations following a steam flow disturbance could thus be predicted and minimized. The fact that the system disturbance (steam flow) is measurable also makes the MPC design favorable over techniques such as $H^\infty$ control where the disturbances are assumed to be a worst case scenario.

We also have the possibility to use an MPC as a high level controller. The MPC would here give offset values to the current controllers in order to improve the system performance. This would in turn allow for a high level of security if parts of the MPC were to fail. A zero output from the MPC would in this case only return the system to the current design. The major points for and against using an MPC design are;

+ Using the design presented in figure 4.8 it will be possible to implement the MPC in addition to the existing control system. This would preserve some if the safety aspects of the current system.

+ The controller should be able to improve performance at both steam flow- and FCV DP disturbances.

+ The MPC design has the possibility to incorporate the actuator limits in the control signal optimization algorithm.

− As was the case for the decoupling filter the controller performance will be dependant on internal model accuracy, although the MPC will allow for more complex models to be used.

− The MPC algorithm is quite large and has a higher demand on computing power than conventional controllers. This is mainly an effect of using "on line" optimization of the control signal. The MPC could thus not be implemented on the current control aperture available at the plant.

### 4.4.3 Suggested controller / MPC

The overall conclusion from this chapter is that an MPC controller would be most suitable for the task of improving the current system. Both for its ability to meet most of our demands but also for the way it can be implemented on top of the current control system. The suggested controller can be seen in figure 4.8. The main reason for picking the flow reference as a controlling point is the fact that we don't have to worry about the derivative part of the SG level controller. The feed forward of the feed water flow would also make it unfeasible to put the controlling point after the SG flow controller, which in that case would try to counteract every move made by the MPC.

The next step is to determine if the solution is feasible using the simulation model of the plant. This means that we need a model of the MPC controller. The following chapter will thus be covering the design process of the MPC controller and its Dymola implementation.

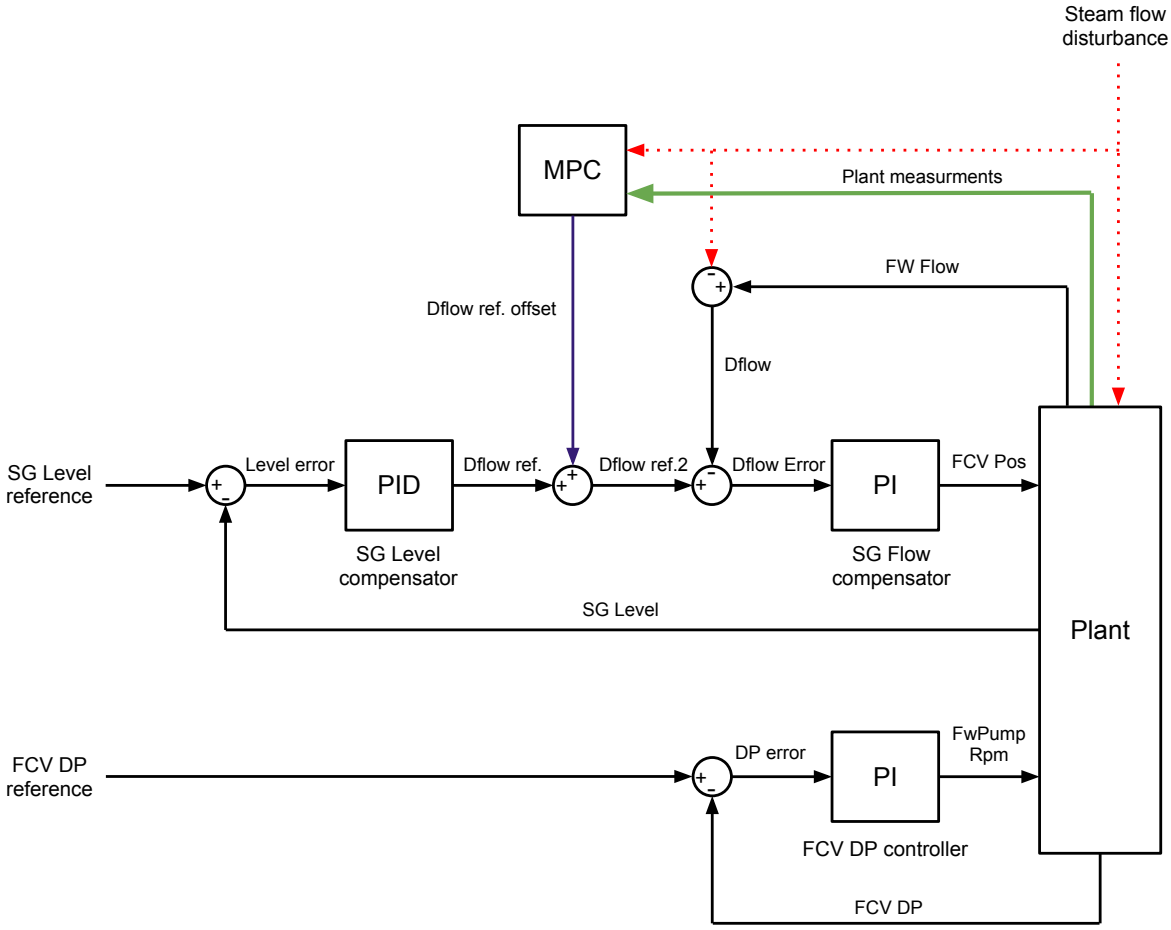


Figure 4.8: Overview of the control system with the suggested MPC controller. The plant will in this case represent the parts of the real plant that will be modelled in the MPC internal model. The green line representing the plant measurement will consist of FCV DP, SG water level and feed water flow.

# Chapter 5

# MPC controller design

The purpose of this chapter is to present the design and evaluating process of the MPC controller suggested in the previous chapter. Due to the scope of the project the design will be fairly simple and should only be seen as an indication of a possible improvement strategy.

## 5.1 MPC introduction

The basic idea behind MPC is to use a simulation model in order to predict the impact of a certain control signal, hence the name model predictive control. The controller is usually based on a discrete time algorithm. At each sampling instant information about the "real" plant is gathered through measurements which then are used as input data for the internal model. The model is used to calculate the future response of the plant which in turn is used to optimize the control signal. The control optimization is dependent mainly on two parameters, the prediction horizon ($N_p$) and the control horizon ($N_c$). The prediction horizon specifies how many samples into the future of the plant response should be used in the optimization. Similarly the control horizon determines how many of the future control signals should be included in the optimization. The control optimization is performed "on line" at every sampling instant. This type of MPC is often referred to as receding horizon control "RHC" due to the moving time window.

The MPC algorithm at each sample can be summarized in the following way:

1. Gather measurement data from the "real" plant.
2. Update the internal model to match the measurements.
3. Determine optimal control signals for $N_c$ samples into the future. The optimization will use the response of the model over the prediction horizon.
4. Send out the new control signal.

### 5.1.1 MPC models

The performance of the controller will depend mainly on the accuracy of the internal model. Depending on the plant and existing information of the plant different types of model may be used. Usually models attained from some type of system identification technique are used to approximate the plant. There are however cases where more intricate models based on the physical structure of the plant are favorable. The MPC algorithm is also capable of handling nonlinear models which makes it more versatile than most other control strategies. In this thesis a reduced linear model attained from the existing Dymola model will be used.

## 5.2 MPC theory/design

The field of MPC control theory is quite extensive due to the flexibility of the MPC design structure. There are numerous books and papers written on the subject of both theory and implementation of

MPC controllers. Due to the scope of the project a fairly simple discrete design using a state space representation of the internal model has been used. A lot of the underlying theory and implementation has been based on the structure presented in the book "Model Predictive Control and Design Using MATLAB" by Grimble M. et al., [18]. The book "Model Predictive Control" by Camacho E.F. et al. [19] has also been used to give a broader view into the field of MPC and how to handle MPC design with measurable disturbances.

### 5.2.1 MPC internal model

As have been mentioned earlier the goal of the controller is to regulate the SG water level by manipulating the SG level controller flow reference. We also have a disturbance in the system in the form of changes in the steam flow outlet from the SG. The model we need for the MPC should thus have flow reference offset as input ($u_1$) and the steam flow as a disturbance input ($u_2$). The output from the model should be the SG water level ($y_1$), we will here also add the FCV DP and feed water flow as outputs ($y_2$ and $y_3$). It will be shown later that these parameters can be used to improve the state update procedure.

Since we already have a fairly accurate model of the plant constructed in Dymola it seems reasonable to use that model as a starting point for the MPC internal model. It is however not possible to use the Dymola model directly due to it's high complexity which would make the MPC to slow too keep up with a reasonable sampling frequency. Instead a simplified version of the model has been constructed without the reactor. The visual representation of the model can be seen in appendix A.4. Using an inbuilt function in Dymola it is then possible to linearize the model at a nominal steady state point where $u_1 = 0$, $u_2 = 552$, $y_1 = 69$, $y_2 = 8$ and $y_3 = 552$. The extracted model is attained in standard state space form as:

$$\dot{x} = Ax + Bu \tag{5.1}$$
$$y = Cx + Du \tag{5.2}$$

where $u = \begin{bmatrix} u_1 & u_2 \end{bmatrix}^T$, $y = \begin{bmatrix} y_1 & y_2 & y_3 \end{bmatrix}^T$ and $D = 0$ in our case. The model is however still large with about 50 states. Model order reduction techniques using balance realization has therefore been used in MATLAB. The basic concept of the reduction is to remove as many states as possible while still attaining a good approximation of the relationship between input and output. The resulting model has 15 states which is within reasonable limits to be used in the MPC. During the reduction the $D$ matrix will differ from zero although at the 15 state level the contribution of $Du$ on the output is small enough to be neglected, the reason for this is that the MPC theory does not allow for direct influence on the output by the input.

Since the MPC used in this thesis will be of discrete type the model also needs to be discretized. This is done using the zero order hold technique in MATLAB with a sampling time of 1 second. The sampling time has been chosen to suit the need for accuracy and stability of the model while still be long enough to avoid unnecessary computations in the MPC. The last step is to split the $B$ matrix to separate the normal input ($u_1$) from the disturbance input ($u_2$), here renamed $u$ and $v$. The model can now be written as

$$x_m(k_i + 1) = A_m x_m(k_i) + B_m u(k_i) + V_m v(k_i) \tag{5.3}$$
$$y_m(k_i) = C_m x_m(k_i) \tag{5.4}$$

where $k_i$ is used to denote a specific sample.

#### 5.2.1.1 Model augmentation

The discrete nature of the MPC algorithm is well suited for using incremental changes in variables instead of absolute values. We thus want to transform our model to fit this specification. By applying the shift operator to equation 5.3 and 5.4 we get

$$x_m(k+1) - x(k) = A_m(x_m(k) - x_m(k-1)) + B_m(u(k) - u(k-1)) + V_m(v(k) - v(k-1)) \tag{5.5}$$
$$y_m(k) - y_m(k-1) = C_m(x_m(k) - x_m(k-1)). \tag{5.6}$$

here $k_i$ is replaced with $k$ to shorten the notation. We can now make the following substitutions; $\Delta x_m(k) = x_m(k) - x_m(k-1)$, $\Delta u(k) = u(k) - u(k-1)$ and $\Delta v(k) = v(k) - v(k-1)$. The substitution

is not made for $y_m$ since we are interested in the absolute value of these parameters. Equation 5.6 can now be rewritten as $y_m(k) = C_m\Delta x_m(k) + y_m(k-1)$. $y_m$ will thus depend on both the current $\Delta x_m$ and the previous absolute value of $y_m$. To keep track of previous $y_m$ we introduce a new state variable $x(k) = \begin{bmatrix}\Delta x_m(k) & y_m(k)\end{bmatrix}^T$. The "update" equation for the $y_m$ state can be written as:

$$\begin{aligned} y_m(k+1) &= C_m\Delta x_m(k+1) + y_m(k) && (5.7)\\ &= C_m((A_m\Delta x_m(k) + B_m\Delta u(k) + V_m\Delta v(k)) + y_m(k) && (5.8)\end{aligned}$$

Using the new state variable the augmented model can be written as

$$\underbrace{\begin{bmatrix}\Delta x_m(k+1)\\ y_m(k+1)\end{bmatrix}}_{x(k+1)} = \underbrace{\begin{bmatrix}A_m & \varnothing\\ C_mA_m & \mathbf{I}\end{bmatrix}}_{A}\underbrace{\begin{bmatrix}\Delta x_m(k)\\ y_m(k)\end{bmatrix}}_{x(k)} + \underbrace{\begin{bmatrix}B_m\\ C_mB_m\end{bmatrix}}_{B}\Delta u(k) + \underbrace{\begin{bmatrix}V_m\\ C_mV_m\end{bmatrix}}_{V}\Delta v(k). \quad (5.9)$$

The augmented output equation is divided into two parts, one to attain the output variable we want to control (SG level) $y_c$ and one equation to attain all the observable outputs (FCV DP, SG level and feed water flow) $y_{ob}$.

$$y_c(k) = \underbrace{\begin{bmatrix}\varnothing & 1 & 0 & 0\end{bmatrix}}_{C}\begin{bmatrix}\Delta x(k)\\ y_m(k)\end{bmatrix} \quad (5.10)$$

$$y_{ob}(k) = \underbrace{\begin{bmatrix}\varnothing & \mathbf{I}^{3\times3}\end{bmatrix}}_{H}\begin{bmatrix}\Delta x(k)\\ y_m(k)\end{bmatrix} \quad (5.11)$$

The resulting augmented model will be able to handle incremental values while still giving the correct absolute value on the output. This has been accomplished to the cost of adding one state for each output.

#### 5.2.1.2 Augmented model validation

Before we can use the augmented model we first need to make sure that it will give the correct output to a certain input and that the discretization process did not affect the system to much. The augmented model has therefore been simulated in Simulink MATLAB and validated against data from the Dymola model (see appendix A.4). The result of using a sampling interval of 1 second can be seen in figure 5.1. We can clearly see that model give a good estimate of the behavior following a steam flow disturbance. There are however differences in the peak values for both the SG level and the FCV DP graphs. This is mainly due to the nonlinear relation between FCV DP and feed water flow that we saw in equation (3.3). This relation is approximated with a linear equation around the steady state point when the linearization of the Dymola model is performed. The approximation will thus be less accurate farther away from the steady state value which is exactly what we see here. The mismatch will affect the prediction capability of the controller but is still deemed to be accurate enough to be used.

### 5.2.2 Model state update

One of the most important steps in the MPC algorithm is to keep the model states updated. This step is vital since the model is only a rough approximation of the real plant (which we saw in the previous section) and will inevitably drift away from the real plant. Since the states in our model can't be measured directly we instead have to use an observer to estimate the states values from plant measurements. The estimated version of the state variable will be denoted by $\hat{x}$. At a specific sampling instant we can gather measurements from the real plant and update our $y_{ob}$ variable to match these. By then forming the difference between the updated $y_{ob}(k)$ and the calculated version $H\hat{x}(k)$ we can update all the model states by multiplying the difference with an observer gain matrix $K_{ob}$ (or Kalman matrix in this case). The update equation will have the following form

$$\hat{x}(k+1) = A\hat{x}(k) + B\Delta u(k) + V\Delta v(k) + K_{ob}(y_{ob}(k) - H\hat{x}(k)). \quad (5.12)$$

The next step is to determine the observer gain matrix $K_{ob}$ in a way that will give a good state estimation. Assume that we have uncontrollable measurement disturbances ($w$) and model state errors ($s$)

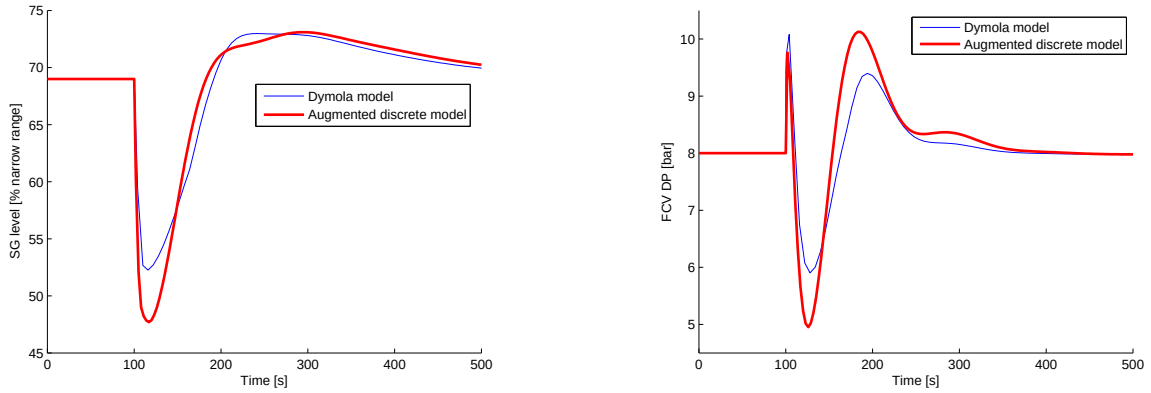


Figure 5.1: SG level (left) and FCV DP response (right) in the augmented 18 state discrete model (red) and the Dymola model (blue) following a 200 kg/s decrease in steam flow at $t = 100$ s.

corresponding to white gaussian noise (WGN) in the following way

$$x(k+1) = Ax(k) + B\Delta u(k) + V\Delta v(k) + s(k) \tag{5.13}$$
$$y_{ob}(k) = Hx(k) + w(k) \tag{5.14}$$

where $s \sim WGN(0,R)$, $w \sim WGN(0,Q)$ and the cross spectrum between $s$ and $w$ is assumed to be zero. Using the noise variances $R$ and $Q$ we can calculate the gain matrix based on the error covariances using the Kalman technique (see page 137 in the book "Control Theory" by Glad T. and Ljung L. [20]). Since all of the states in our model are detectable from the output the observer gain can be calculated via the discrete Ricatti equation in the following way

$$K_{ob} = APH^T(HPH^T + Q)^{-1} \tag{5.15}$$

where

$$P = APA^T - APH^T(HPH^T + Q)^{-1}HP^TA^T + R. \tag{5.16}$$

The remaining task is to determine the $R$ and $Q$ variance matrices to give the best state estimate. The general guide line is that high variance will indicate a large portion of disturbance in the signal which in turn will make the measurement less trustworthy. Dimensioning the variances will be discussed further in the parameter tuning section (5.2.6).

### 5.2.3 Output prediction

The heart of the MPC algorithm is the optimization of the control signal. As was mentioned in the MPC introduction the optimization is to be performed by evaluating the response of the internal model. This can be done in several ways depending on the demands on the controller and type of model. The simplest form of optimization can be applied when dealing with linear models with no constraints. In many cases most of the computation associated with the optimization can be performed "off line" in order to reduce the MPC iteration time.

The first step toward finding the optimal control is to calculate the future output of the model within the prediction window ($N_p$). To do this we first need to find the future state values.

$$\tilde{x}(k+1|k) = Ax(k) + B\Delta u(k) + V\Delta v(k) \tag{5.17}$$
$$\tilde{x}(k+2|k) = Ax(k+1) + B\Delta u(k+1) \tag{5.18}$$
$$= A^2x(k) + AB\Delta u(k) + AV\Delta v(k) + B\Delta u(k+1) \tag{5.19}$$
$$\vdots \tag{5.20}$$
$$\tilde{x}(k+N_p|k) = A^{N_p}x(k) \tag{5.21}$$
$$+A^{N_p-1}B\Delta u(k) + A^{N_p-2}B\Delta u(k+1) + \cdots + A^{N_p-N_c}B\Delta u(k+N_c-1) \tag{5.22}$$
$$+A^{N_p-1}V\Delta v(k) \tag{5.23}$$

where $\tilde{x}(k+1|k)$ denotes the predicted value of the state $x(k+1)$ given information available at sample instant $k$. We have here assumed $\Delta v$ is equal to zero for all future measurements since this is an unpredictable disturbance, and $\Delta u$ is equal to zeros for all predictions outside the control horizon ($N_c$). The notation can be simplified by introducing the vectors

$$X = \begin{bmatrix}\tilde{x}(k+1|k) & \tilde{x}(k+2|k) & \cdots & \tilde{x}(k+N_p|k)\end{bmatrix}^T \tag{5.24}$$

$$\Delta U = \begin{bmatrix}\Delta u(k) & \Delta u(k+1) & \cdots & \Delta u(k+N_c-1)\end{bmatrix}^T. \tag{5.25}$$

We can now write the predicted states as

$$X = A_p x(k) + B_p \Delta U + V_p \Delta v(k) \tag{5.26}$$

where

$$A_p = \begin{bmatrix} A \\ A^2 \\ \vdots \\ A^{N_p} \end{bmatrix}; \quad B_p = \begin{bmatrix} B & 0 & \cdots & 0 \\ AB & B & \cdots & 0 \\ \vdots & & \ddots & \\ A^{N_p-N_c} & A^{N_p-N_c-1} & \cdots & B \\ A^{N_p-N_c-1} & A^{N_p-N_c-3} & \cdots & AB \\ \vdots & & & \vdots \\ A^{N_p-1}B & A^{N_p-2}B & \cdots & A^{N_p-N_c}B \end{bmatrix} \tag{5.27}$$

$$V_p = \begin{bmatrix} V \\ AV \\ \vdots \\ A^{N_p-1}V \end{bmatrix}. \tag{5.28}$$

The predicted output can now be attained using equation 5.11. Every matrix element in equation 5.26 should thus be multiplied by the C matrix to get the predicted output vector $Y$.

$$Y = Fx(k) + \Phi \Delta U + \Psi \Delta v(k) \tag{5.29}$$

where

$$Y = \begin{bmatrix}\tilde{y}(k+1|k) & \tilde{y}(k+2|k) & \cdots & \tilde{y}(k+N_p|k)\end{bmatrix}^T \tag{5.30}$$

$$F = \begin{bmatrix} CA \\ CA^2 \\ \vdots \\ CA^{N_p} \end{bmatrix}; \quad \Phi = \begin{bmatrix} CB & 0 & \cdots & 0 \\ CAB & CB & \cdots & 0 \\ \vdots & & \ddots & \\ CA^{N_p-N_c} & CA^{N_p-N_c-1} & \cdots & CB \\ CA^{N_p-N_c-1} & CA^{N_p-N_c-3} & \cdots & CAB \\ \vdots & & & \vdots \\ CA^{N_p-1}B & CA^{N_p-2}B & \cdots & CA^{N_p-N_c}B \end{bmatrix} \tag{5.31}$$

$$\Psi = \begin{bmatrix} CV \\ CAV \\ CA^2V \\ \vdots \\ CA^{N_p-1}V \end{bmatrix} \tag{5.32}$$

We now have the ability to predict the output (SG water level) with the internal model using equation 5.29.

### 5.2.4 Control optimization

The first step in optimizing the control signal is to establish an objective function which should be minimized. The primary goal of the controller is to keep the output variables as close to the reference

as possible. We thus start by forming the objective function $J$ using the square of the reference error as the parameter to minimize.

$$J = (Y - R_y)^T (Y - R_y) \tag{5.33}$$

$R_y$ is a vector containing the reference ($r_y$) for the predicted outputs, in our case zeros since the model we are using has been normalized around its steady state value. There is however also favorable to add a term penalizing large changes in the control signal. There might otherwise be problems with unrealistically large values. In this case we will use the weight matrix ($R_u \geq 0$) on the control variables within the control horizon and add this to the objective function.

$$J = (Y - R_y)^T (Y - R_y) + \Delta U^T R_u \Delta U \tag{5.34}$$

$R_u$ is a identity matrix with weights in the diagonal corresponding to the different control signals. In our case the same weight ($r_u$) will be used for all future signal. To avoid integrator wind up in the SG level controller we also add a term penalizing the MPC control signal amplitude which in turn will drive the output back to zero after a transient has passed. This is done by using the actual value of the current output signal ($u(k-1)$) multiplied with a scaling factor $a_w$ and $\Delta U$. In order to minimize this term the future control signal changes will have to be opposite that of the current control signal. The final objective function will thus be

$$J = (Y - R_y)^T (Y - R_y) + \Delta U^T R_u \Delta U + u(k-1) A_w \Delta U \tag{5.35}$$

where $A_w$ is a row vector with $a_w$ as scalar elements. Since we are looking to minimize $J$ with respect to $\Delta U$ we continue by writing $Y$ as a function of $\Delta U$ using equation (5.29).

$$\begin{aligned}
J &= (Fx(k) + \Phi \Delta U + \Psi \Delta v(k) - R_y)^T (Fx(k) + \Phi \Delta U + \Psi \Delta v(k) - R_y) && (5.36)\\
&\quad + \Delta U^T R_u \Delta U + u(k-1) A_w \Delta U && (5.37)\\
&= (Fx(k) + \Psi \Delta v(k) - R_y)^T (Fx(k) + \Psi \Delta v(k) - R_y) && (5.38)\\
&\quad + 2\Delta U^T \Phi^T (Fx(k) + \Psi \Delta v(k) - R_y) + \Delta U^T (\Phi^T \Phi + R_u) \Delta U + u(k-1) A_w \Delta U && (5.39)\\
&= f_1(x(k), \Delta v(k)) + \Delta U^T f_2(x(k), \Delta v(k), u(k-1)) + \Delta U^T \tilde{E} \Delta U && (5.40)
\end{aligned}$$

Here the functions $f_1$,$f_2$ and constant $\tilde{E}$ have been added to simplify the notation.

#### 5.2.4.1 Quadratic programming

As was mentioned in the MPC introduction we not only want to minimize the objective function (5.40) we also want to make sure that we keep the control signal within certain limits. To achieve this we need a more intricate strategy of finding the minimum of the objective function rather than just looking at its derivative. In this case we will use an optimization technique called quadratic programming (QP). The basic problem formulation in QP is to minimize the objective function

$$\tilde{J} = \frac{1}{2} x_d^T E x_d + x_d^T L \tag{5.41}$$

subject to a set of constraints

$$M x_d \leq \gamma \tag{5.42}$$

where the minimization is performed with respect to the decision variable $x_d$. The first step is thus to formulate our problem to fit the QP structure. Looking at our objective function (5.40) we see that we can remove the term $f_1(x(k), \Delta v(k))$ since it is not affected by the our decision variable, which in this case is $\Delta U$. We can also treat $f_2(x(k), \Delta v(k), u(k-1))$ as a constant for the same reason. Rewriting the objective function we get

$$\tilde{J} = \frac{1}{2} \Delta U^T E \Delta U + \Delta U^T L \tag{5.43}$$

where $E = 2\tilde{E}$ and $L = f_2(x(k),\Delta v(k))$. The next step is to define the optimization constraint matrices $M$ and $\gamma$. Let's say we want to implement the constraint $c_l \leq \Delta U \leq c_u$, where $c_l$ and $c_u$ are vectors containing the limits for each control signal in $\Delta U$. The matrices will then have the form

$$M\Delta U \leq \gamma \tag{5.44}$$

$$\begin{bmatrix} \mathbf{I} & 0 \\ 0 & -\mathbf{I} \end{bmatrix} \Delta U \leq \begin{bmatrix} c_u \\ c_l \end{bmatrix} \tag{5.45}$$

The algorithm for solving the QP is taken more of less directly from the book "Model Predictive Control and Design Using MATLAB" [18] and have been modified to work in the Dymola environment. It is based on Hildreth's algorithm which is both simple and stable enough to be used in this type of application, it is also a good way to avoid unnecessary matrix inversions which might otherwise cause numerical difficulties. The optimization algorithm has been constructed as a function which has $E$,$L$,$M$,$\gamma$ as inputs and returns the optimal $\Delta U$ vector. The Dymola code for the function can be seen in appendix A.1.

### 5.2.5 Dymola implementation

The Dymola implementation of the MPC controller has been performed with the intention of creating a controller that can be used in different situations and is easy to modify. Most of the calculations have therefore been included in the Dymola code. The only part of the calculation not performed in Dymola is the observer gain matrix calculation. This is due to the fact that there is no readily available solver for discrete algebraic Ricatti equations in Dymola. Instead the observer calculations have been performed in MATLAB using the "dare" solver. This also means that the internal model augmentation has been done in MATLAB since the augmented model is needed in the observer gain calculation.

The input to the MPC controller will thus be the augmented model in the form of the $A$,$B$,$C$,$V$,$H$ and $K_{ob}$ matrices. We also need to specify the prediction horizon ($N_p$) and control horizon ($N_c$) as well as the weights for the control signals, regulated parameters, control signal amplitudes and control signal limits. The controller has been constructed as an extension of the discrete component class in Dymola which will handle the data capturing depending on the sampling time and first sampling instant. An overview of the input parameters in the controller interface can be seen in appendix A.3.

As have been previously mentioned a lot of the calculations in the MPC can be performed "off line" during the initiation process. Dymola code for the "online" iteration performed at each sample (corresponding to the list in section 5.1) can be found in appendix A.2.

### 5.2.6 Controller tuning

Tuning the MPC controller can be quite a formidable task considering the wide range of parameters. A good way is to start from the internal model perspective and work with the other parameters from there.

#### Observer variance matrix Q and R

The first step is to determine suitable values for the variance matrices $Q$ and $R$ that are used in the calculation of the observer gain. They are both diagonal matrices. The $R$ matrix determines the noise variance level for the plant measurements. Since we have no noise in our simulation model we could put this to a very small value. A small value would however give rapid changes in the internal model states which could lead to instability. A good compromise has been to set a larger variance value for the FCV DP and feed water flow measurement while the slower changing SG level can be given a lower value.

$$R = \begin{bmatrix} 10 & 0 & 0 \\ 0 & 0.1 & 0 \\ 0 & 0 & 10 \end{bmatrix} \tag{5.46}$$

The $Q$ matrix is the variance of the model states, since we cannot determine the internal disturbances in this case we will give all states an arbitrary variance of 1, $Q = \mathbf{I}^{18\times 18}$.

**Prediction horizon $N_p$**

The prediction horizon should be picked large enough to cover the settling time of the system. In figure 5.2 and 5.3 we can see two simulations done in MATLAB using the MPC regulator to control a linearized version of the simplified simulation model. It is clear that a short prediction horizon will lead to unwanted performance. In our case the settling time is quite large which was one of the main reasons for choosing a fairly large sampling time of 1 second. Extending the prediction by only increasing the prediction horizon will cause numerical difficulties in the type of predictions algorithm used in this project. A prediction horizon of 60 samples has been shown to be suitable for this implementation, which means that the controller will look one minute into the future.

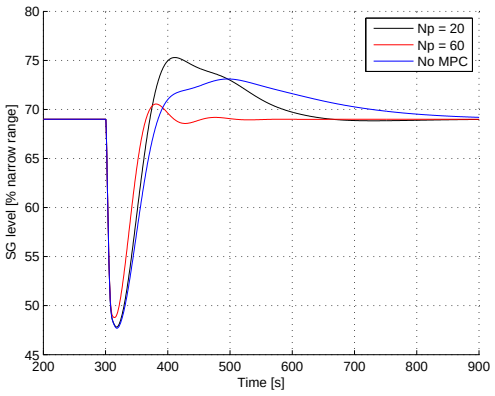


Figure 5.2: MATLAB simulation of a 200 kg/s step decrease in steam flow using the non reduced linear model as simulation.

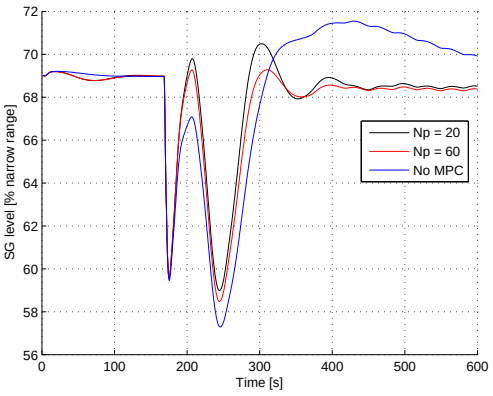


Figure 5.3: MATLAB simulation of the system response following a steam flow disturbance corresponding to a load rejection transient using the non reduced linear model as simulation.

**Control horizon $N_c$ and control penalty $r_u$.**

The control horizon should be picked large enough to give the controller a reasonable chance to stabilize the system using a control signal up to the horizon. A horizon of 45 samples has been shown to be favourable in this case. Coupled with the horizon we also have the control penalty which will determine the amount of control signal used by the controller. The control signal is in this case the incremental $\Delta u$ from the augmented system and not the absolute value. A penalty of 20 will give a reasonably fast response while not inducing to much oscillations.

### Control amplitude weight $A_c$ and limits $u_{max}$, $u_{min}$.

As was mentioned before the aim of the control amplitude weight is to force the controller to a zero output once the transient has passed. The amplitude weight should thus be large enough to allow the system to return in reasonable time but not large enough to influence the performance during the transient. A value of 10 has been used in this case. The output limits has been set to assure that the system does not give rise to too large control signals during unforeseen transients. In this case the control signal has been allowed in the interval $[-7,7]$ which corresponds to a Dflow reference interval of about $[-50,50]$ kg/s.

## 5.3 Simulation results

The simulations have been performed using both the simplified simulation model (see appendix A.6) and the full simulation model. Three types of disturbances have been tested; FCV DP step increase, steam flow step decrease and 50% load rejection where one turbine is stopped.

### 5.3.1 FCV DP step increase

The step increase in FCV DP is induced as a reference change in the FCV DP controller from 8 to 10 bar at $t = 1100$ s. The simulation has been performed using the full simulation model. The SG level during the transient can be seen in figure 5.4. The graphs show a small increase in performance using the MPC design. The MPC output is presented in figure 5.5. It's clear from the results that the MPC works as intended and will try to close the FCV due to the high FCV DP. There is however room for further improvement by tuning the controller to give a faster response. The current maximum MPC output of $-0.4$ corresponds to a decreased flow reference for the SG flow compensator by about 3.5 kg/s.

The impact of the MPC on the FCV DP and FCV position is presented in figure 5.6 and 5.7. The FCV DP response shows a small increase in performance where the overshoot has been eliminated. The same behavior can also be observed in the FCV position graph.

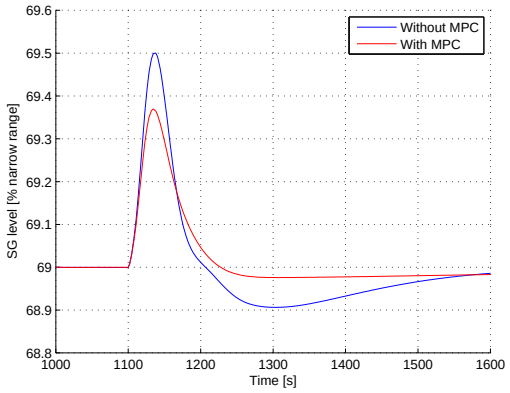


Figure 5.4: SG level during a step increase in FCV DP.

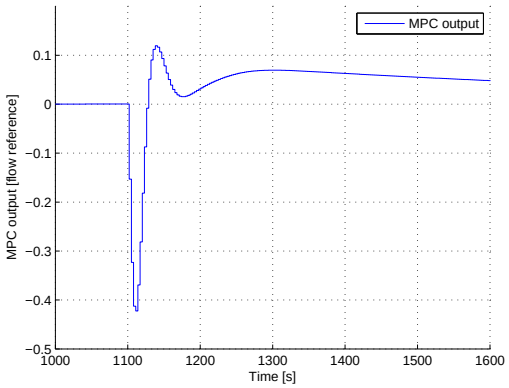


Figure 5.5: MPC output during a step increase in FCV DP.

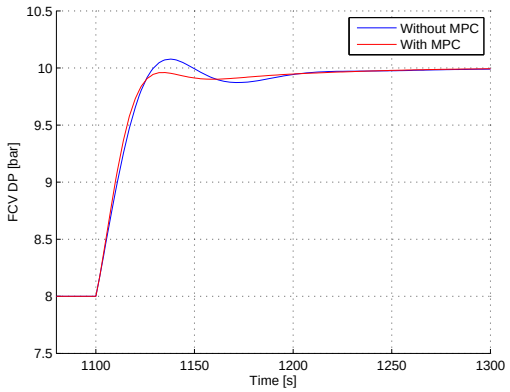


Figure 5.6: FCV DP during a step increase in FCV DP. The plot interval has been scaled to highlight the interesting part of the step response.

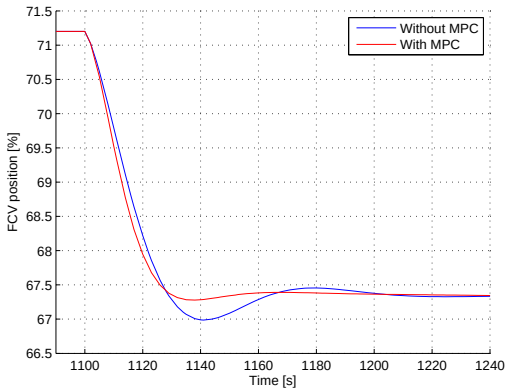


Figure 5.7: FCV position during a step increase in FCV DP. The plot interval has been scaled to highlight the interesting part of the step response.

### 5.3.2 Steam flow step decrease

The steam flow step decrease has been simulated using the simplified simulation model to allow for direct control of the steam flow. The step is induced at $t = 1100$ as a decrease from 550 kg/s to 350 kg/s (flow values for one SG). The SG level and MPC output from the simulations can be seen in figure 5.8 and 5.9. There is a clear improvement in SG level response where a lot of the overshoot has been eliminated due to the compensating behavior of the MPC. The lack of improvement in minimum value is as predicted from the optimal controller case in figure 4.4. From the MPC output graph we can see that the MPC reacts in the appropriate way by initially trying to open the FCV. The output will also try to return to zero once the transient has been settled due to the control signal amplitude weight.

Figure 5.10 and 5.11 show the impact of the new controller on the FCV DP and FCV position. The increased response in FCV position will give rise to larger fluctuations in FCV DP, although they are well within reasonable limits from this project. Interesting to note is also that the MPC is a bit too slow in order to eliminate the drop in FCV position directly after the steam drop.

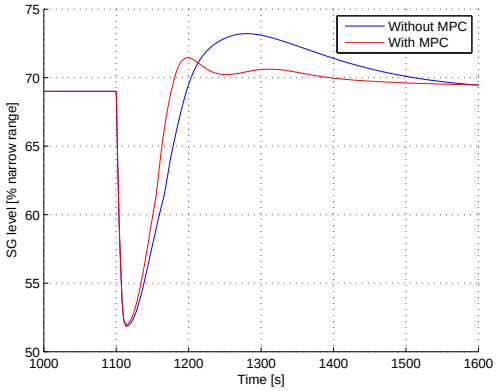


Figure 5.8: SG level during a step decrease in steam flow.

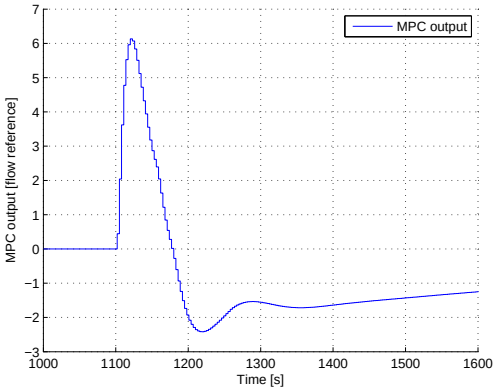


Figure 5.9: MPC output during a step decrease in steam flow. The maximum amplitude of 6 corresponds to a increase in flow reference for the SG flow compensator by 42 kg/s.

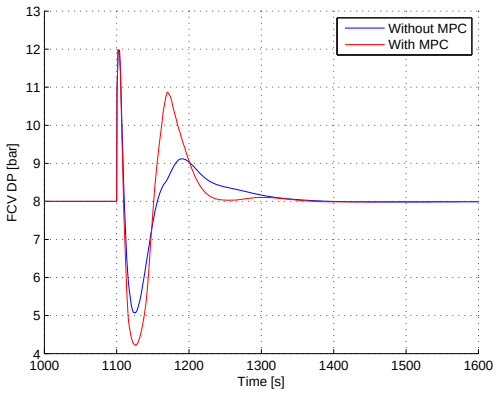


Figure 5.10: FCV DP during a step decrease in steam flow.

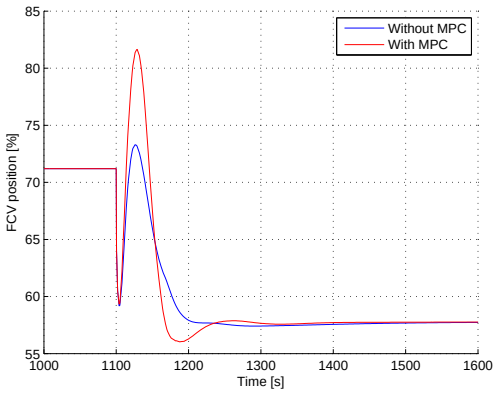


Figure 5.11: FCV position during a step decrease in steam flow.

### 5.3.3 Load rejection (50%)

The 50% load rejection disturbance has been simulated with both the simplified and the full simulation model. The reason for using both models is to see how simplifications in the model will affect the controller performance.

The disturbance is induced as a reference step in turbine power at $t = 3167$ s in one of the turbines. The SG level response from the simplified model is presented in figure 5.12. There is a clear improvement in response when using the MPC where a lot of the overshoot has been eliminated. The level does however have some difficulties returning to the reference value due to overcompensation by the MPC. In figure 5.13 we see that the MPC will have a decreasing output after the main transient has passed, this is an effect of the slow ramping down in steam flow that follows this type of disturbance. The MPC overestimates the impact of the ramping on the SG level and will thus cause the level to remain below the reference until the steam flow is stabilized. The MPC output graph also indicates that the output limits of $[-7,7]$ are enforced by limiting the second output peak.

The final test for the MPC is a 50% load rejection disturbance in the full simulation model. Initial simulations with the previous control penalty resulted in oscillatory behavior of the SG level. The problem was determined to be approximations done in the internal model which neglect the effect of reduced RC temperature on the SG level dynamics. An increased control penalty of 150 was able to give a stable system response which can be seen in figure 5.14. The corresponding MPC output graph is presented in figure 5.15 where the effect of the increased penalty can be seen in the reduced MPC output amplitude. This will of course also limit the beneficial impact of the controller on the system. Ways to improve the current design are presented in chapter 6.

The FCV DP and FCV position during the disturbance for both models are presented in figures 5.16 to 5.19. It is easy to see that a higher control activity in the MPC will lead to larger transients in the FCV DP. This behavior is caused by the increased reaction in FCV position.

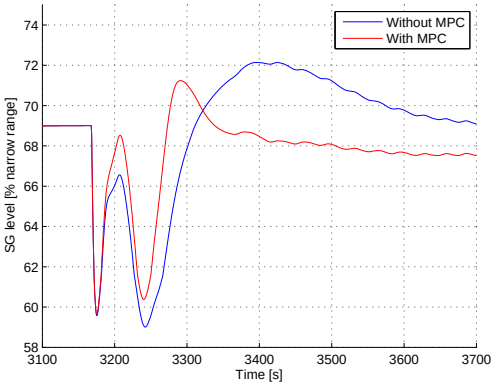


Figure 5.12: SG level during a 50% load rejection disturbance using the simplified simulation model.

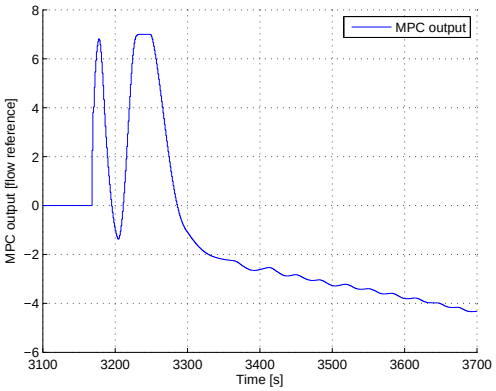


Figure 5.13: MPC output during a 50% load rejection disturbance using the simplified simulation model. The maximum amplitude of 7 corresponds to an increase in flow reference for the SG flow compensator by 50.5 kg/s.

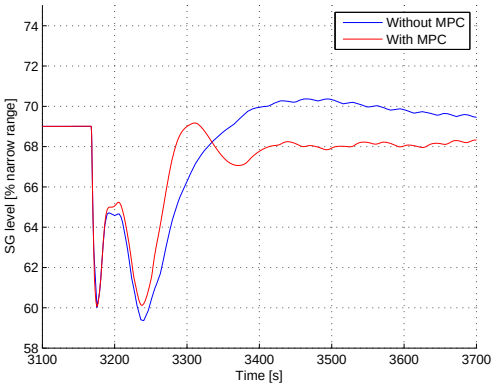


Figure 5.14: SG level during a 50% load rejection disturbance using the full simulation model and a control penalty of 150.

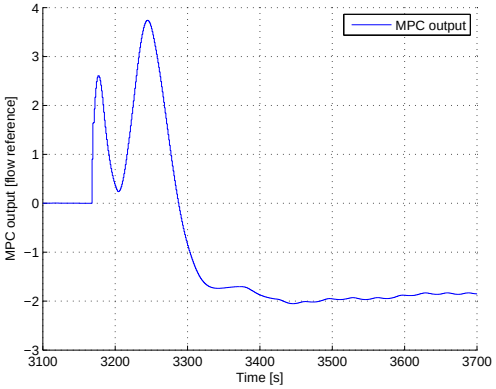


Figure 5.15: MPC output during a 50% load rejection disturbance using the full simulation model and a control penalty of 150. The maximum amplitude of about 3.5 corresponds to an increase in flow reference for the SG flow compensator by 25 kg/s.

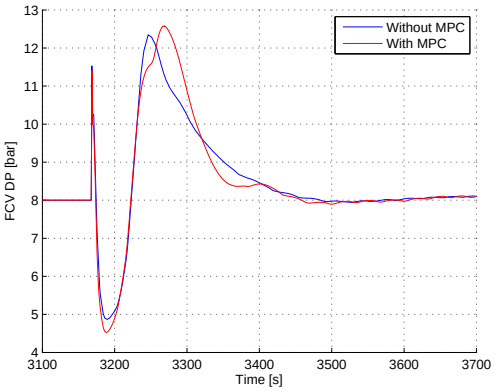


Figure 5.16: FCV DP during a 50% load rejection disturbance using the full simulation model and a control penalty of 150.

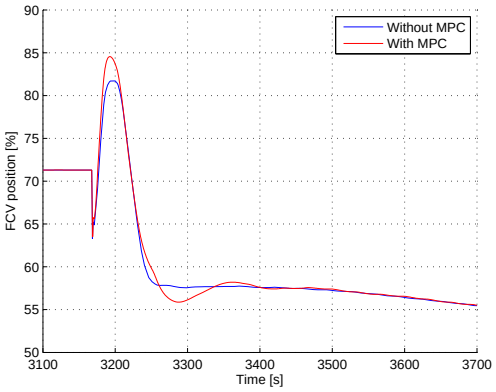


Figure 5.17: FCV position during a 50% load rejection disturbance using the full simulation model and a control penalty of 150.

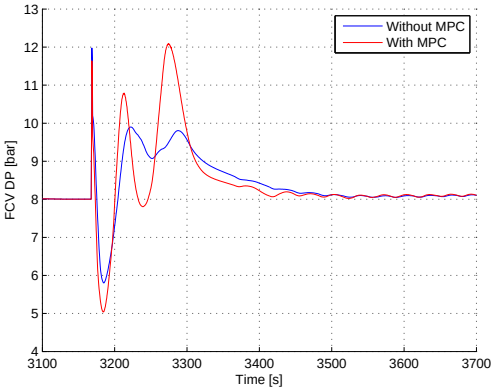


Figure 5.18: FCV DP during a 50% load rejection disturbance using the simplified simulation model.

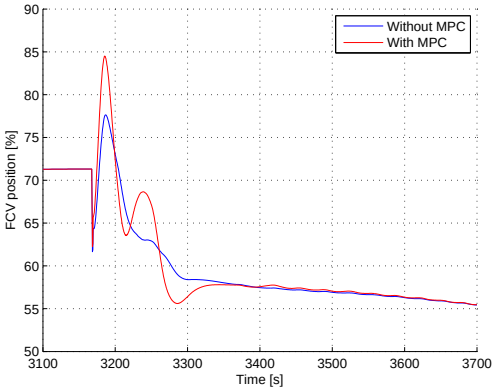


Figure 5.19: FCV position during a 50% load rejection disturbance using the simplified simulation model.

# Chapter 6

# Discussion

## 6.1 Simulation model results and improvements

The simulation model showed a good resemblance to data collected in the real plant, there are however a few things that could be improved in order to attain a better simulation result. For one the FCV friction is completely neglected in the model which results in a somewhat misleading simulation result. The oscillations originating from the FCV could in worst case be amplified by the controller to create system instability. This type of behavior cannot be evaluated using the model in its current form.

## 6.2 MPC results discussion

The main goal for the MPC design process and implementation was to see if the control system could be improved while still maintaining a good safety level. The results show that the system performance can be improved even though the improvements are fairly small. The controller objectives for the SG level are met in the case of overshoot and damping. This does however not mean that the controller is ready or viable for implementation in the current state. Additional tuning and modifications needs to be performed before the controller performance can be deemed satisfactory. One also needs to keep the cost in mind when looking for implementation possibilities. As has been shown in this report the increase in control performance of using this type of controller is fairly small which has to be related to the productivity increase in the plant. In this case less down time caused by, for example, high water level in the SG would lead to higher productivity, the question is if it's high enough to justify this type of controller. A stable controller might also lessen the wear on valves and other actuators which in turn would require less maintenance.

Is there any guarantee that the controller will work in the real plant based solely on the simulation results? The short answer to this question is that there is no such guarantee. The simulation results presented in this report should only be viewed as a indication of the system response. There are a lot of additional questions that need to be addressed before any implementation can be performed.

### 6.2.1 MPC modifications and suggestions

The design task was some what limited by the restriction of implementing the MPC "behind" the current controllers. This also meant that the drop in feed water flow following a load rejection disturbance could not be eliminated completely. There is also a problem with integrator wind up in the SG level compensator which forces the MPC to compensate even more to avoid a big overshoot. A better solution would probably be to remove the level compensator completely and let the MPC determine the flow reference to the SG flow compensator. This configuration would however not have the same level of redundancy if the MPC were to shut down.

The MPC controller presented in the project is based directly on a state space model of the plant, this direct approach will lead to numerical difficulties for large prediction horizons. This was one of the factors leading to the fairly large sampling interval of 1 second for the internal model. In general a shorter interval would be favorable to get the correct system response. The model response was however

validated for different inputs and was deemed to be satisfactory. An alternative of using a large sampling interval can be to use a model description based on Laguerre functions which was suggested in the later chapters of the book "Model Predictive Control and Design Using MATLAB" by Grimble et al. [18]. By using a decreasing weighting of future control signals and model outputs the prediction horizon can be chosen large enough to mimic an infinite horizon. This would also lead us to a control law corresponding to an LQR structure which would allow for a more extensive stability analysis.

#### 6.2.1.1 Internal model improvements

The main reason for the limited performance of the MPC controller is most likely the quality of the internal model. It is not always easy to find a good balance between model complexity and system performance. In this case the system could probably benefit from a more extensive internal model to incorporate the RC and reactor dynamics. A few tests were performed using the RC and feed water temperatures as disturbance inputs which indicated that this might be a possible way to improve the system. To increase the performance in the FCV DP disturbance case a closer link between the measured FCV DP and the MPC would probably be desirable.

The most radical improvement would be to use a nonlinear model to base the MPC predictions on. The MPC could in this case be designed to compensate for the static friction in the FCV's. The nonlinear model would however require a more computational demanding optimization procedure which could limit the sampling frequency.

# Chapter 7

# Conclusion

The project has resulted in a model of the plant at Ringhals 3 that has been validated against measurement data. The validation has been performed for three different transients; FCV DP disturbance, SG level disturbance and 50% load rejection disturbance. Simulation results show that the model is a good approximation of plant and in particular the feed water system and SG's.

The current control system has been analyzed where the main weakness was determined to be the response to a steam flow drop and FCV DP coupling to the SG water level. An initial solution using feed forward of the FCV DP signal was evaluated with limited success. The most promising solution was instead to implement an MPC controller in connection to the existing controllers. Simulations results using the MPC controller showed a small increase in system performance which could most likely be improved by using some of the suggestions made in the previous chapter.

# Bibliography


[1] B.-G. Bergdahl and R. Oguma, "Reglering av matarvattenflödet i en PWR," tech. rep., GSE Power Systems AB, February 2007.

[2] F. Zhao, J. Ou, and W. Du, "Simulation modeling of nuclear steam generator water level process - a case study," ISA Transactions, vol. 39.

[3] J. Schlichting, "Ringhals 3 Turbine PLS (Precautions, Limitations and Setpoints)," tech. rep., Ringhals AB, September 2009.

[4] "Ånggeneratorernas reglering och mätning R3," tech. rep., KSU AB and Ringhals AB, 2002.

[5] J. Schlichting, "Ringhals 3 Reactor PLS (Precautions, Limitations and Setpoints)," tech. rep., Ringhals AB, January 2010.

[6] M. Stepniewski, "Input data for a computer model verification of the Ringhals 3 steam generator," tech. rep., Ringhals AB, May 2005.

[7] "Ånggeneratorernas reglering och mätning R3," tech. rep., KSU AB and Ringhals AB, October 2002.

[8] "Processreglering och skydd övergripande 540," tech. rep., KSU AB and Ringhals AB, October 2002.

[9] A. B. Nordquist, "Dynamic modelling of a nuclear reactor system," Master's thesis, Chalmers University of Technology and Solvina AB, may 2006.

[10] A. Nordquist, "Model validation report," tech. rep., Solvina AB, May 2006.

[11] A. Egeholm and B. Lundberg, "Provrapport, Kontrol av varvtalsstyrda matarvattenpumpar," tech. rep., Ringhals AB, August 2009.

[12] A. Nordquist, "Provrapport, Kontrol av ånggeneratorernas nivåreglering," tech. rep., Ringhals AB, October 2009.

[13] B. Lennartson, Reglerteknikens grunder. Studentlitteratur, 2002.

[14] A. G. Parlos and I. T. Rais, "Nonlinear control of U-tube steam generators via $H_\infty$ control," Control Engineering Practice, vol. 8.

[15] K. Hu and J. Yuan, "On switching $H_\infty$ controllers for nuclear steam generator water level: A multiple parameter-dependent Lyaponov functions approach," Annals of Nuclear Energy, vol. 35.

[16] Z. Dong, X. Huang, and J. Feng, "Water-Level Contol for the U-Tube Steam Generator of Nuclear Power Plants Based on Output Feedback Dissipation," IEEE Transactions on Nuclear Science, vol. 56, June 2009.

[17] C. Liu, F. Y. Zhao, P. Hu, P. Hu, and C. Li, "P controller with partial feed forward compensation and decoupling control for the steam generator water level," Nuclear Engineering and Design, vol. 240.

[18] M. J. Grimble and M. A. Johnson, Model Predictive Control and Design Using MATLAB©. Springer-Verlag London, 2009.

[19] E. F. Camacho and C. Bordons, Model Predictive Control. Springer-Verlag London, 2004.

[20] T. Glad and L. Ljung, Control Theory, Multivariable and Nonlinear Methods. Taylor and Francis, 2000.

# Appendix A

# Dymola implementation

## A.1 Hildreth's quadratic programming

The Dymola code for the optimization algorithm used in the MPC controller can be seen in figure A.1. The first step in the optimization is to determine if any of the constraints are violated, if not, the optimization will be performed as a simple matrix equation. The level of computation needed in each iteration is thus in close relation to the number of active constraints.

The Dymola function *Modelica.Math.Matrices.solve()* has been used to avoid most matrix inversions which are less favourable due to their numerical instability.

```
function QuadProgram
  input Real E[:,size(E,1)];
  input Real F[size(E,1),1];
  input Real M[:,size(E,1)];
  input Real gamma[:,1];
  output Real DU[size(E,1),1];

protected
  Real H[size(gamma,1),size(gamma,1)];
  Real K[size(gamma,1),1];
  Real lambda[size(gamma,1),1];
  Real lambda_p[size(gamma,1),1];
  Real error;
  Real w;
  Boolean ActiveConstraint=false;
  Boolean OptimNotDone=true;

algorithm
  DU := -matrix(Modelica.Math.Matrices.solve(E,vector(F))); // E * DU = -F
  for i in 1:size(gamma,1) loop
    if scalar(M[i,:]*DU) > gamma[i,1] then
      ActiveConstraint := true;
    end if;
  end for;

  if ActiveConstraint then
    H := M*Modelica.Math.Matrices.inv(E)*transpose(M);
    K := gamma + M*Modelica.Math.Matrices.inv(E)*F;
    lambda :=  zeros(size(gamma,1),1);

    for k in 1:40 loop
      if OptimNotDone then
        lambda_p := lambda;

        for i in 1:size(gamma,1) loop
          w := (-1/H[i,i])* ( K[i,1] + scalar(H[i,:]*lambda) - H[i,i]*lambda[i,1]);
          lambda[i,1] := max(0,w);
        end for;

        error := scalar(transpose(lambda-lambda_p)*(lambda-lambda_p));
        if error <= 10^(-8) then
          OptimNotDone := false;
        end if;

      else
      end if;
    end for;
    //DU := DU - Modelica.Math.Matrices.inv(E)*transpose(M)*lambda;
    DU := -matrix(Modelica.Math.Matrices.solve(E,vector(F+transpose(M)*lambda))); //E * DU = -F-M'
  end if;
```

Figure A.1: Dymola code for the optimization algorithm.

## A.2 MPC ”online” calculations

At each sampling instant the controller will run the code presented in figure A.2. The $E$, $M$, $F2$, $F3$ and $F4$ matrices are determined ”off line” in the initiation process.

```
when sampleTrigger then
  // Step 1: Gather plant measurements
  Dv = v-pre(v); // Form the disturbance input Dv

  // Step 2: Update internal model to match the measurements (y)
  xe = A*pre(xe) + B*Du + V*Dv + Kob*(y - H*pre(xe));

  // Step 3: Calculate optimal control signal
  for i in 0:Nu-1 loop // Calculate gamma matrix
    for k in 1:size(B,2) loop
      gamma[i*size(B,2)+k,1] =  umax[k]-u[k];
      gamma[i*size(B,2)+k+Nu*size(B,2),1] =  -umin[k]+u[k];
    end for;
  end for;
  L = matrix(F2*xe) + matrix(F3*Dv) + matrix(F4*u); // Calculate L matrix
  DU = QuadProgram(E,L,M,gamma); // Optimization of the control signal using quadratic program
  Du = DU[1:size(B,2),1]; // Only the first sample will be used as control signal

  // Step 4: Send out the new control signal
  u = pre(u) + Du;
end when:
```

Figure A.2: Dymola code executed at each MPC iteration.

## A.3 MPC interface

The MPC interface in Dymola can be seen in figure A.3. The number of controller inputs and outputs are linked to the dimensions of the $H$, $V$ and $B$ matrices. Control penalties and output constraints can be set for each individual output. This project did however only utilize one output.

The matrices describing the internal model ($A$,$B$,$C$,$D$,$H$,$V$) and observer gain matrix $Kob$ can be transferred directly from MATLAB using the Dymola m-function library. The function *tsave.m* will convert matrices in MATLAB to a format that can be read by Dymola.

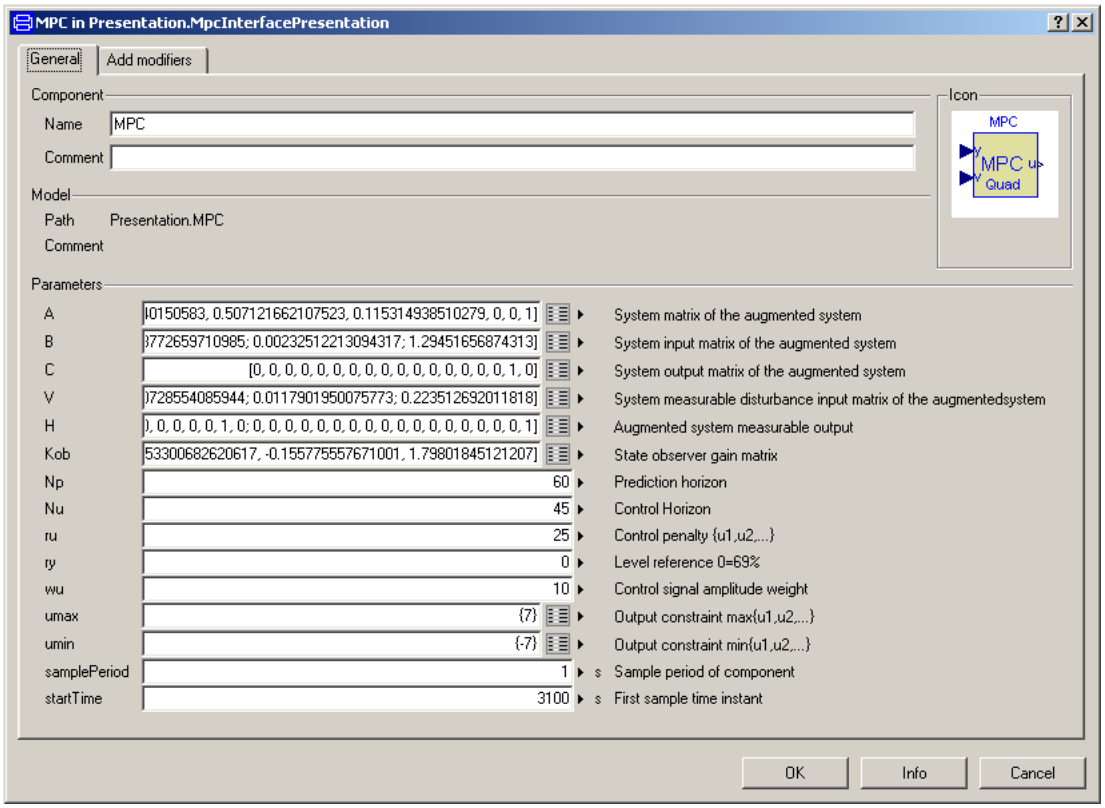


Figure A.3: Input parameters for the MPC controller in Dymola.

## A.4 MPC internal model basis

As have been previously mentioned the internal model used in the MPC is a discretized reduced linear version of a nonlinear Dymola model, which can be seen in figure A.4. The model is run to a steady state corresponding to a 100% plant power level at which the linearization is performed using the inbuilt Dymola linearizer.

The reactor and turbines have been replaced by constant boundary flows to simplify the model. There is also only one SG used which is feed by a single feed water lane. The flows have been scaled to compensate for the lower number of components. The linearized version has 52 state variables which is a significant reduction from the 254 state variables in the full simulation model.

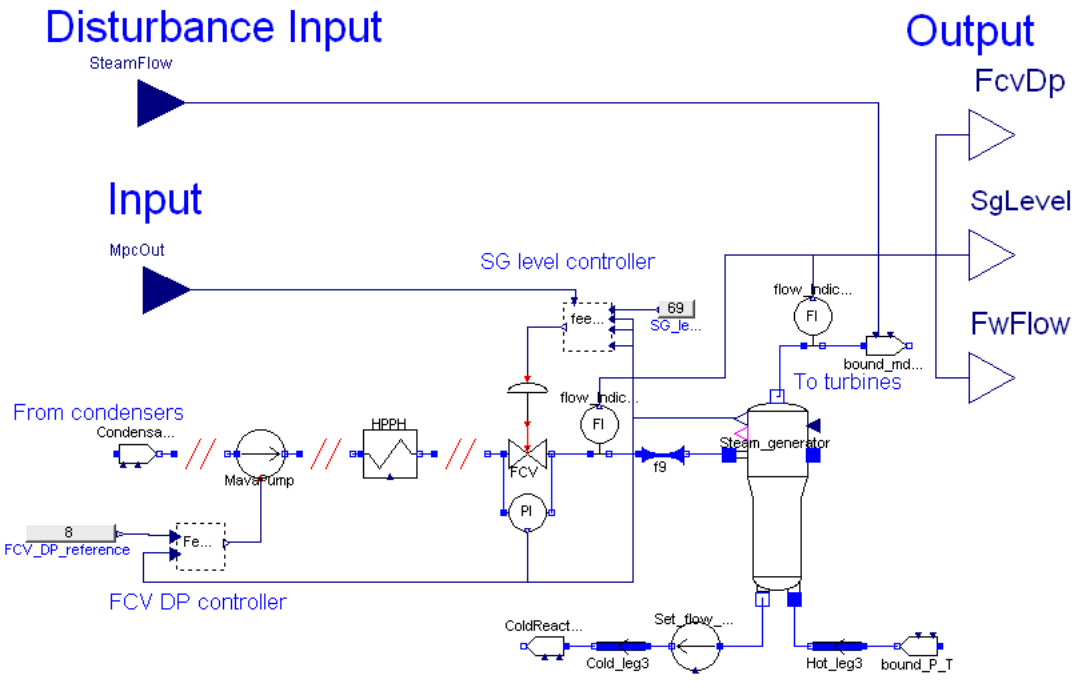


Figure A.4: Dymola model used as basis for the MPC internal model.

## A.5 SG level and FCV DP controllers

The Dymola implementation of the SG level and FCV DP controllers can be seen in figure A.5 and A.6. Measurement values are scaled to match signal levels in the real plant.

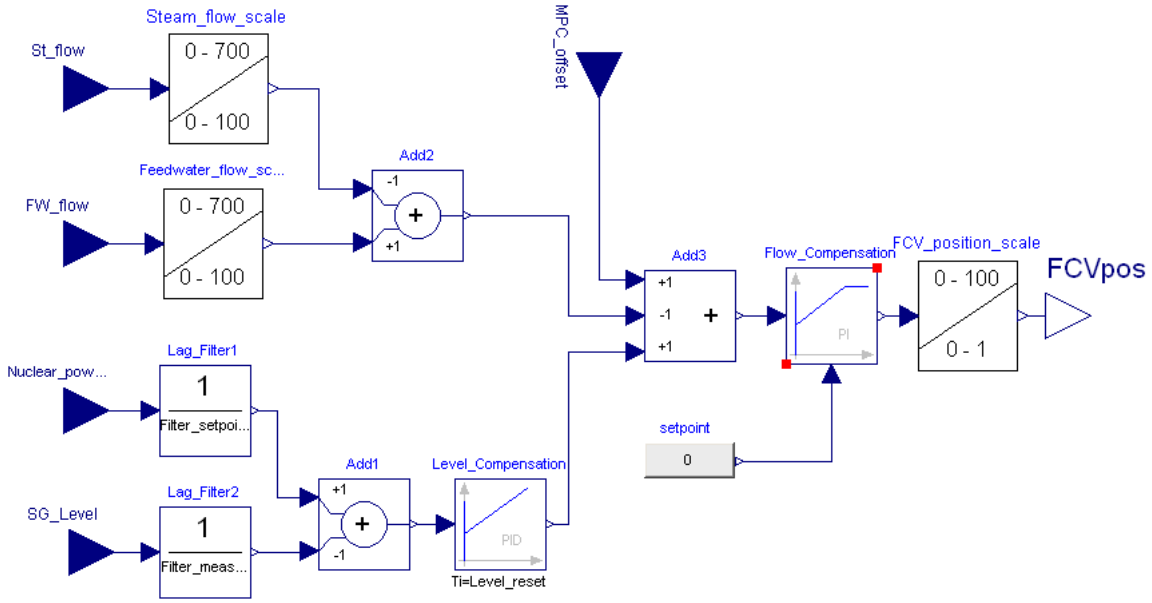


Figure A.5: SG level controller with the added input for the MPC controller.

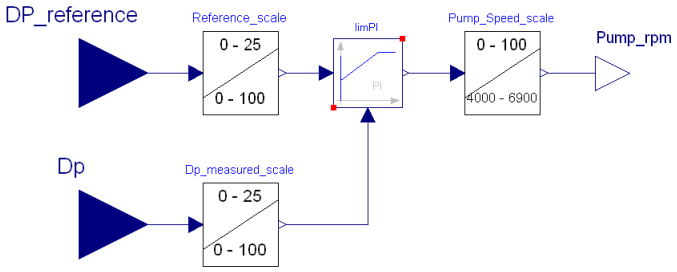


Figure A.6: FCV DP controller.

## A.6 Simplified simulation model with MPC

The simplified simulation model seen in figure A.7 is a slightly more complex version of the MPC internal model basis seen in the previous section. Here the turbine models used in the full simulation model has been added to allow for simulation of the load rejection disturbance. The MPC is connected to the SG level controller in the way presented in figure 4.8.

Measurements signals routed to the MPC has been normalized around their steady state values since the linearised internal model in the MPC only handles perturbations around the linearization point.

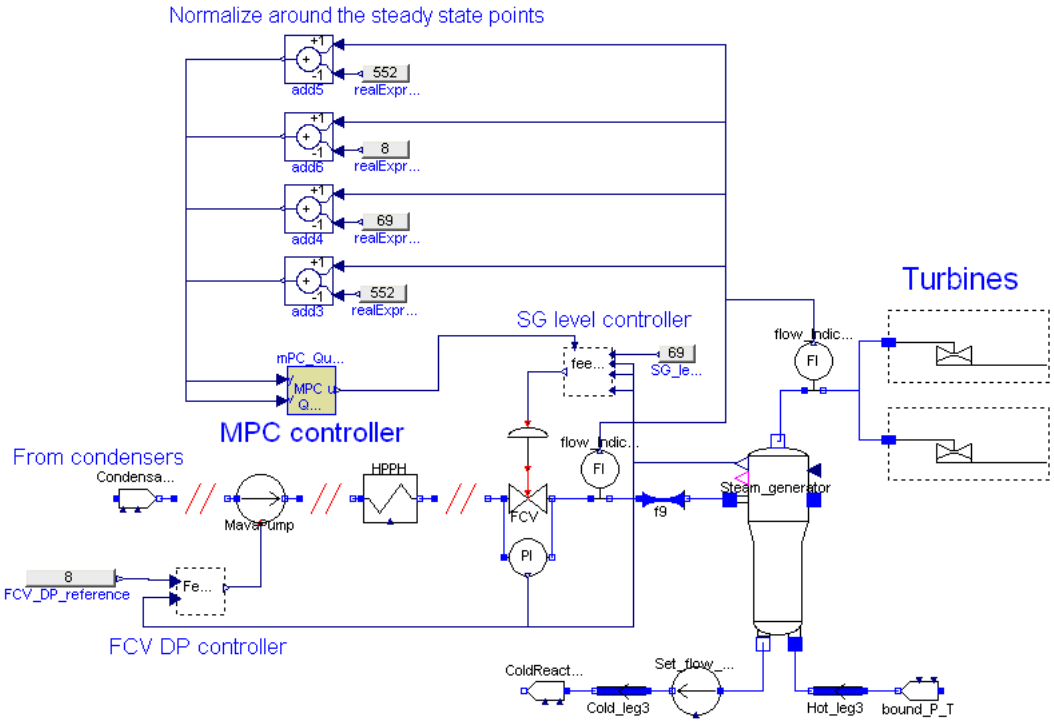


Figure A.7: The simplified simulation model and MPC controller.